remote sensing

MDPI

Review

Review of Land Surface Albedo: Variance Characteristics, Climate Effect and Management Strategy

Xiaoning Zhang [1,2,3], Ziti Jiao [1,2,*], Changsen Zhao [3], Ying Qu [4], Qiang Liu [1], Hu Zhang [5], Yidong Tong [1,2], Chenxia Wang [1,2], Sijie Li [1,2], Jing Guo [1,2], Zidong Zhu [1,2], Siyang Yin [1,2] and Lei Cui [5]

1 State Key Laboratory of Remote Sensing Science, Beijing Normal University, Beijing 100875, China; xnzhang@bnu.edu.cn (X.Z.); toliuqiang@bnu.edu.cn (Q.L.); tongyd@mail.bnu.edu.cn (Y.T.); wangchenxia@mail.bnu.edu.cn (C.W.); lisijie@mail.bnu.edu.cn (S.L.); guojing0404@mail.bnu.edu.cn (J.G.); zhuzidong@mail.bnu.edu.cn (Z.Z.); yinsy@mail.bnu.edu.cn (S.Y.)
2 Beijing Engineering Research Center for Global Land Remote Sensing Products, Institute of Remote Sensing Science and Engineering, Faculty of Geographical Science, Beijing Normal University, Beijing 100875, China
3 College of Water Sciences, Beijing Normal University, Beijing 100875, China; zhaochangsen@bnu.edu.cn
4 Key Laboratory of Geographical Processes and Ecological Security in Changbai Mountains, Ministry of Education, School of Geographical Sciences, Northeast Normal University, Changchun 130024, China; quy100@nenu.edu.cn
5 School of Geographic and Environmental Sciences, Tianjin Normal University, Tianjin 300387, China; huzhang@tjnu.edu.cn (H.Z.); cuil@mail.bnu.edu.cn (L.C.)
* Correspondence: jiaozt@bnu.edu.cn

Abstract: Surface albedo plays a controlling role in the surface energy budget, and albedo-induced radiative forcing has a significant impact on climate and environmental change (e.g., global warming, snow and ice melt, soil and vegetation degradation, and urban heat islands (UHIs)). Several existing review papers have summarized the algorithms and products of surface albedo as well as climate feedback at certain surfaces, while an overall understanding of various land types remains insufficient, especially with increasing studies on albedo management methods regarding mitigating global warming in recent years. In this paper, we present a comprehensive literature review on the variance pattern of surface albedo, the subsequent climate impact, and albedo management strategies. The results show that using the more specific term "surface albedo" is recommended instead of "albedo" to avoid confusion with similar terms (e.g., planetary albedo), and spatiotemporal changes in surface albedo can indicate subtle changes in the energy budget, land cover, and even the specific surface structure. In addition, the close relationships between surface albedo change and climate feedback emphasize the important role of albedo in climate simulation and forecasting, and many albedo management strategies (e.g., the use of retroreflective materials (RRMs)) have been demonstrated to be effective for climate mitigation by offsetting CO_2 emissions. In future work, climate effects and management strategies regarding surface albedo at a multitude of spatiotemporal resolutions need to be systematically evaluated to promote its application in climate mitigation, where a life cycle assessment (LCA) method considering both climate benefits and side effects (e.g., thermal comfort) should be followed.

Keywords: surface albedo; radiative forcing; global warming; climate feedback; vegetation; soil; snow–ice; water; urban; carbon trade-off

Citation: Zhang, X.; Jiao, Z.; Zhao, C.; Qu, Y.; Liu, Q.; Zhang, H.; Tong, Y.; Wang, C.; Li, S.; Guo, J.; et al. Review of Land Surface Albedo: Variance Characteristics, Climate Effect and Management Strategy. *Remote Sens.* **2022**, *14*, 1382. https://doi.org/10.3390/rs14061382

Academic Editor: Maruthi Sridhar Balaji Bhaskar

Received: 17 January 2022
Accepted: 10 March 2022
Published: 12 March 2022

1. Introduction

Surface albedo is defined as the ratio of the reflected irradiance in the viewing hemisphere to the total incident solar irradiance [1,2], which plays an essential role in surface energy balance, carbon and water cycling, medium- to long-term climate and weather forecasting, and global change studies [3,4]. In the Paris Agreement, the ambitious goal to restrict global warming to 2 °C and preferably close to 1.5 °C relative to preindustrial times (i.e., the mid-nineteenth century) by the end of the 21st century was created, and this goal

requires rapid and sustained decarbonization, especially before the assumed emissions peak by 2030 [5,6]. Human-induced warming reached an estimated 0.93 °C ± 0.13 °C above mid-nineteenth-century conditions in 2015, is currently increasing by nearly 0.2 °C per decade [7], and increased to 1.07 °C in 2019, as recently reported in the Intergovernmental Panel on Climate Change (IPCC) AR6 [8]; thus, there is a limited window in which to develop a more carbon-efficient future for climate mitigation. Implementation requirements were recommended for the Global Climate Observing System (GCOS) sponsored by the World Meteorological Organization (WMO) with a view towards the Sustainable Development Goals (SDGs) and the implementation of the Paris Agreement, where surface albedo is listed as one of the Essential Climate Variables (ECVs) in the terrestrial biosphere domain in a phased 5–10 year implementation plan published in 2016 [9]. The IPCC AR6 highlights the intensity and frequency of hot temperature extremes over land due to continuous global warming dozens of times and calls for mitigation decisions rather than passive adaptation [10].

Numerous algorithms and products regarding surface albedo have been developed for decades and are widely applied in resolving climate problems. Bidirectional reflectance distribution function (BRDF) angular modelling [11] and narrow-to-broadband conversions [12] are the two main processes involved in surface albedo retrieval from satellite observations under cloudless conditions, and a series of surface albedo products have been generated, ranging from those of 250 m to 20 km, daily to monthly, and 5 to 30 years in spatial resolution, temporal resolution and temporal span, respectively [13], such as the Moderate Resolution Imaging Spectroradiometer (MODIS) [11] and Global Land Surface Satellite (GLASS) [14] surface albedo product. A general accuracy requirement of 0.02–0.05 is recommended within 5–10 years on a global scale [1,2], and a smaller uncertainty of ±0.02 for regional climate simulation is required [3]. Based on these mature algorithms and datasets, many studies have focused on monitoring the spatiotemporal variance in global surface albedo, as well as its effect on perturbations in Earth's radiative balance—or radiative forcing and climate feedback. Surface albedo presents different patterns over various land surfaces and their seasonable transformation [15], including soil, vegetation, urban areas, ice, snow and water surfaces. Subsequently, the change in surface albedo can affect heat and moisture exchange between the land surface and atmosphere, and a positive radiative forcing would lead to an increase in temperature [16], ice melt [17], snow melt [18] and vice versa. To address these problems, many climate intervention strategies have been implemented to offset anthropogenic climate change, especially for global warming [19,20].

At present, several studies have reviewed surface albedo in some directions. First, the primary definition [21], algorithm and product [13] and surface validation [22,23] were reviewed. Then, several studies focused on the variance characteristics over main land cover types, including forest [24], urban [25], snow-covered [26,27] and ice-covered areas [26,28]. In addition, the effect of surface albedo on climate responses was also summarized, including its application in climate simulation [2] and the relationship between surface albedo and CO_2 emission [29]. Moreover, studies on surface albedo in a special ultraviolet (UV) waveband were also reviewed [30]. However, reviews of a single land type generally lack an overall understanding of surface albedo for research, and increasing attention has been placed on the albedo-induced climate feedback under the background of global warming [26,31] and corresponding albedo strategies for climate mitigation [20,32] in recent years. Thus, it is necessary to provide an overview of surface albedo over various land types and its impact on climate change as well as management methods, which will enhance the application potential of surface albedo in climate governance for both researchers and decision makers.

In this paper, we present a comprehensive literature review of the variance pattern of surface albedo over typical land types and special objects, subsequent effects on climate, and albedo management strategies for mitigating these undesirable effects. First, several definitions related to "albedo" are introduced to avoid confusion and distinguish surface albedo from other research objects, and a literature analysis is presented. Second, we review

the spatiotemporal patterns of typical land covers, mixed types and special surfaces. Then, short-to-long-term albedo monitoring and the application and management of these monitoring techniques are summarized. In addition, the main findings, some inconsistencies, and future work are discussed, and our conclusions are presented.

2. Literature Analysis of Surface Albedo

In this study, the literature data were collected from the Web of Science core database, Thomson Reuters. First, we searched for articles and reviews including "albedo" in the titles published from 1 January 1900 to 31 December 2021, resulting in 3287 items in total. However, many articles retrieved focused on similar albedo variables instead of on surface albedo, and thus the data were carefully and manually screened by reading the titles and abstracts. Therefore, we first introduced easily confused definitions related to "albedo", and statistical results involving surface albedo were visualized with visual analysis software.

2.1. Definition Distinction

Figure 1 shows major albedo variables associated with the surface, top of atmosphere (TOA), atmosphere, and cloud layers, where cloud albedo makes a major contribution to Earth's albedo [4]. Moreover, albedo in other fields is also described.

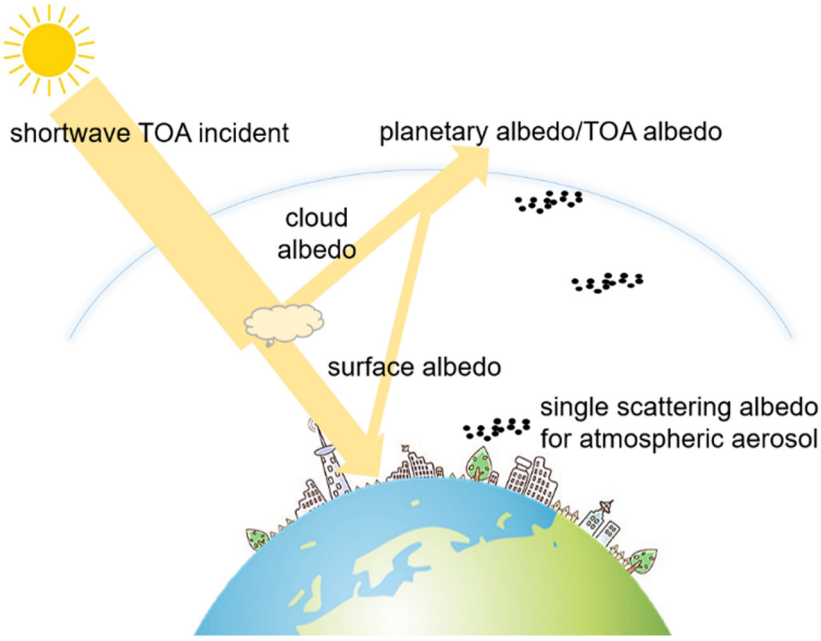

Figure 1. The scenario for several essential albedo variables.

Numerous studies have been carried out on surface albedo over the decades, and it has been defined differently between early [1] and recent research stages [21]. In the field of remote sensing, a recent rigorous definition is provided by [4]: "Surface shortwave broadband albedo represents the surface hemispheric reflectivity integrated over the solar spectrum (0.2–5 μm)". Surface albedo is an important variable in surface energy balance, which can be expressed by Equation (1) [4]. The surface all-wave net radiation R_n represents the balance between incoming radiation from the atmosphere and outgoing radiation from the Earth's surfaces, which is a sum of shortwave net radiation ($R_n{}^s$) and longwave net radiation ($R_n{}^l$). α_{sw} and $F_d{}^s$ refer to surface shortwave broadband albedo and shortwave downward irradiance, respectively. In longwave downward ($F_d{}^l$) and upwelling radiation variables ($F_u{}^l$), ε, T_s, and σ refer to surface longwave broadband emissivity, surface skin temperature, and Stefan–Boltzmann's constant, respectively.

$$R_n = R_n^s + R_n^l = (1 - \alpha_{sw})F_d^s + F_d^l - F_u^l = (1 - \alpha_{sw})F_d^s + \varepsilon F_d^l - \sigma\varepsilon T_s^4 \quad (1)$$

Currently, satellite data provide a unique way to retrieve α_{sw} at large scales, which relies on satellite-acquired basic quantity of reflectance that characterizes (geometrically) the reflecting properties of a specific surface. Considering the natural surface is intermediate between rough Lambert with isotropic diffuse reflection and smooth surface with specular reflection, the intrinsic reflectance anisotropy (i.e., BRDF) of a natural surface is useful primarily as an underlying concept of reflectance [33]. BRDF is defined as the ratio of increments from reflected radiance to that from incident solar irradiance over a tiny surface element at viewing and solar geometries, respectively. Solar irradiance involved in BRDF refers to the incident radiant flux onto a surface element dA, and reflected radiance represents the radiant flux over the projected area of dA at a "conical" solid angle of reflection. Consequently, directional reflectance varies with incident and reflected geometries (i.e., solar zenith angle (SZA, θ_i), view zenith angle (VZA, θ_v), and relative azimuth angle (RAA, φ)) and spectrum wavelength λ. Before the retrieval, satellite-observed TOA reflectances at limited sun-viewing geometries are always transferred into surface reflectances by eliminating atmospheric effects [34], and then the entire BRDF change can be reconstructed by models [11]. To derive the albedo from reflectance measurements, the directional hemispherical albedo (i.e., black-sky albedo (BSA)) and bihemispherical albedo (i.e., white-sky albedo (WSA)) are computed using Equations (2) and (3) [35], which are further combined to measure blue-sky albedo weighted by a percentage of diffuse skylight S as shown in Equation (4) as a function of aerosol optical depth (AOD) [36,37]. Finally, Equation (5) shows the integration of blue-sky albedos from bands λ_1 to λ_2 to obtain shortwave broadband albedo at band Λ. In practice, narrowband-to-broadband conversion coefficients are always utilized to simplify this process based on albedos at several typical narrow bands (e.g., blue, green, red, near-infrared (NIR)), and coefficients for multiple sensors onboard polar orbit and geostationary satellites have been proposed and widely used [12,38–40].

$$\mathrm{BSA}(\theta_i, \lambda) = \frac{1}{\pi} \int_0^{2\pi} \int_0^{\frac{\pi}{2}} R(\theta_i, \theta_v, \varphi, \lambda) \sin\theta_v \cos\theta_v d\theta_v d\varphi \tag{2}$$

$$\mathrm{WSA}(\lambda) = 2 \int_0^{\frac{\pi}{2}} \mathrm{BSA}(\theta_i, \lambda) \sin\theta_i \cos\theta_i d\theta_i \tag{3}$$

$$\alpha(\theta_i, \lambda) = (1 - S(\theta_i, \tau(\lambda)))\mathrm{BSA}(\theta_i, \lambda) + S(\theta_i, \tau(\lambda))\mathrm{WSA}(\lambda) \tag{4}$$

$$\alpha_{sw}(\theta_i, \Lambda) = \frac{\int_{\lambda_1}^{\lambda_2} {F_d}^s(\theta_i, \lambda)\alpha(\theta_i, \lambda)d\lambda}{\int_{\lambda_1}^{\lambda_2} {F_d}^s(\theta_i, \lambda)d\lambda} \tag{5}$$

Then, shortwave radiative forcing from surface albedo change can be calculated to evaluate its climate effect [29]. Given the asymmetry between solar irradiance and the seasonal cycle of surface albedo in many extratropical regions, the local annual mean instantaneous shortwave radiative forcing $RF_{\Delta\alpha}$ at TOA (in $\mathrm{W/m^2}$) is usually estimated following monthly surface albedo changes. One method is to use radiative kernels derived from global climate models [41] although they are model- and state-dependent, and a simplified $RF_{\Delta\alpha}$ model allowing greater flexibility surrounding the prescribed atmospheric state has recently been presented as Equation (6) [42]: where $\Delta\alpha_m$, ${F_d}^s{}_m$, and $T_{m,t}$ refer to a surface albedo change, the incident solar irradiance at surface level, and the all-sky monthly mean clearness index in month m and year t, respectively.

We can see that a negative value can be obtained as surface albedo increases, which shows a cooling effect to offset CO_2 emission. In turn, reduced surface albedo means the exacerbation of warming effect. This circulation is always called surface albedo feedback [27]. Considering importance of snow and sea ice with high albedo, feedbacks over these two kinds of surfaces have been widely studied, which are called as snow albedo feedback (SAF) [27] and sea-ice albedo feedback (SIAF) [32]. Meanwhile, the impact of

albedo feedback on climate change is always focused on, and thus the word "climate feedback" is also widely used [43].

$$RF_{\Delta\alpha}(t) = \frac{1}{12}\sum_{m=1}^{12}\left(-{F_d}^s{}_{m,t}\sqrt{T_{m,t}}\Delta\alpha_{m,t}\right) \quad (6)$$

During literature retrieval, we found that some similar albedo variables may have created confusion. The fraction of incoming solar energy scattered back to space by Earth is referred to as planetary albedo, which is also called Earth albedo or TOA albedo [44,45]. Single scattering albedo (SSA) is generally associated with particles, where atmospheric aerosols near the surface, tropopause and TOA have attracted much attention [46]. Cloud albedo is also called plane parallel albedo and can be mainly affected by cloud-condensation nuclei of dimethyl sulphide, which is produced by marine phytoplankton and chemically oxidizes in the atmosphere to form sulphate aerosols [47,48]. In addition, albedos for special surfaces have also been examined, such as albedos of water bottom [49] and exoplanets [50]. Meanwhile, albedos at special wavelengths have also been investigated [51]. Different from most satellite observations with a passive remote sensing mode depending on solar illumination, an object's albedo from an active light source is also widely used, such as the neutron albedo of a person [52] and metals [53]. In particular, the albedo tissue of fruit peels is extensively used in the food industry [54], especially that from citrus.

Planetary albedo can significantly affect surface temperature [55], and both atmospheric and surface albedos contribute to planetary albedo [56]. Novel stratospheric aerosol injections have been proposed to increase planetary albedo and mitigate global warming [57]. Similarly, the influence of surface albedo variances on planetary albedo needs to be studied in the future. After the above data cleaning, 1714 literatures remained, including 1702 articles and 12 review papers. Therefore, the more specific term "surface albedo" or other kinds of albedo should be included among titles and keywords to avoid confusion.

2.2. Literature Analysis

The 1714 papers focused on surface albedo were imported into bibliometric and visual analysis software HistCite [58] and into VOSviewer for citation statistics and analysis with a focus on publication volume, citations, research fields, citation connections, and keywords.

Publications and total citations associated with surface albedo from 1954 to 2021 are shown in Figure 2, where the publications and citations show a similar increasing trend, especially after 2008. Increased research interest indicates the importance of surface albedo and strengthens confidence in its further investigation.

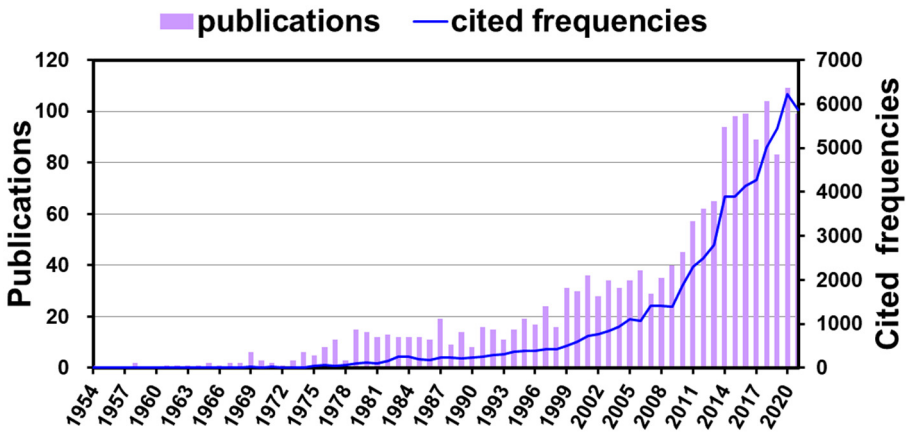

Figure 2. Publications and total cited frequencies associated with surface albedo from 1954 to 2021.

The percentages of research fields are shown in Figure 3. A paper may be related to one or several research areas, and there are 3031 fields for all the 1714 papers. The meteorology atmospheric sciences is the top field that contributes to surface albedo (i.e.,

20.0%). Meanwhile, much attention has also been focused with a proportion of larger than 4.7% in the next six fields, including environmental sciences ecology, geology, remote sensing, imaging science photographic technology, engineering and physical geography. Then, 12 fields account for 17.9% of total selected papers with a percentage from 0.5% to 3.0%, where different surface types (e.g., agriculture, water, ocean, forestry and building) and subjects (e.g., geochemistry geophysics, energy, optics, computer and materials) are included. Overall, surface albedo plays an essential role in various research areas, especially for atmospheric and environmental sciences.

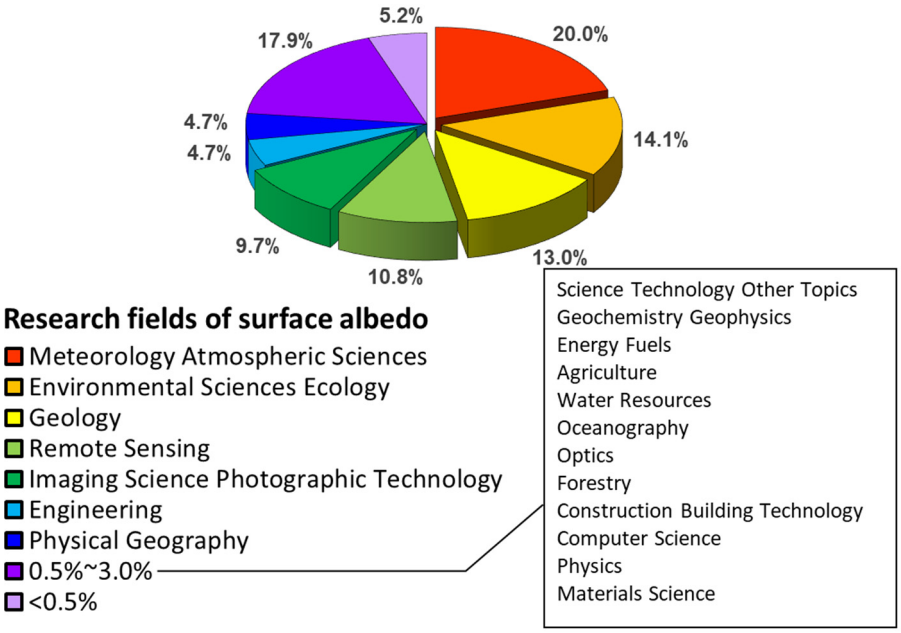

Figure 3. Pie chart of research fields associated with surface albedo.

The relationships between citation connections, research hotspots and institutions were analysed with VOSviewer software. Citation connections are shown in Figure 4, where 538 papers were included with a citation frequency of greater than 30. There are six major cluster networks in total: (1) algorithms, products and validations of surface albedo over various land surfaces at regional and global scales, such as the MODIS surface albedo product [11], and climate analysis, such as urban heat islands (UHIs) [59] and carbon budgets [60] (red dots); (2) definition and inversion algorithms [1,12] (green dots); (3) application to climate analysis, such as drought [61] (blue dots); (4) sea surface albedo [62,63] (light green dots); and (5) and (6) ice and snow albedo and their effects on climate feedback [64,65] (cyan and purple dots).

Research hotspots are shown in Figure 5, which presents the leading 148 items that occur more than 15 times among all 4304 keywords. We can see that the keyword "albedo" achieves the highest density, followed by "climate", "model" and "MODIS", which indicates numerous efforts made in surface albedo-induced climate feedback and inversion algorithms, especially based on the MODIS dataset. The next most significant keywords are "BRDF", "algorithm", "product", "validation", "snow", "vegetation" and "temperature". This shows the important role of primary BRDF characteristics in albedo estimation [11,66,67], and a series of algorithms and products have been developed in previous studies [13]. Notably, albedos of snow [68] and vegetation [69] surfaces have also attracted much attention in global warming research, and surface albedo-induced climate feedback shows an effect on temperature change. In addition, surface albedo has also connected to various land–atmosphere mass and energy exchange processes, such as soil, ocean, mass balance, carbon, atmospheric aerosol, and precipitation processes.

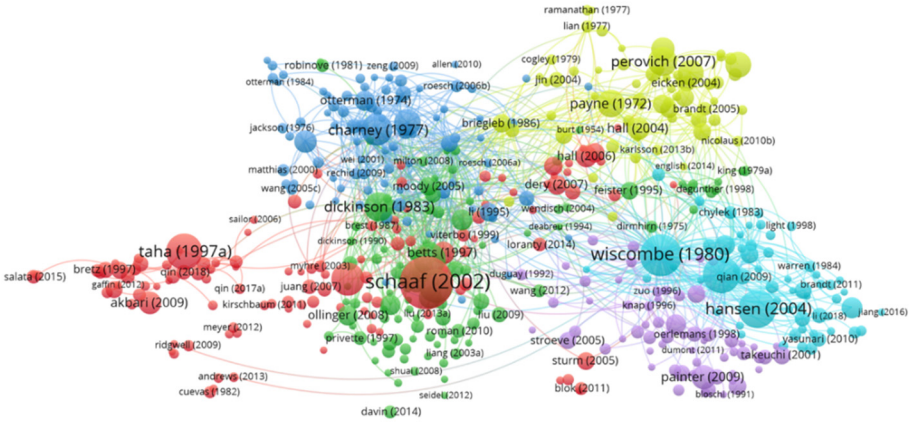

Figure 4. Citation connections for highly cited papers. Colours indicate different clusters with similar research subjects, and sizes vary with citation frequency.

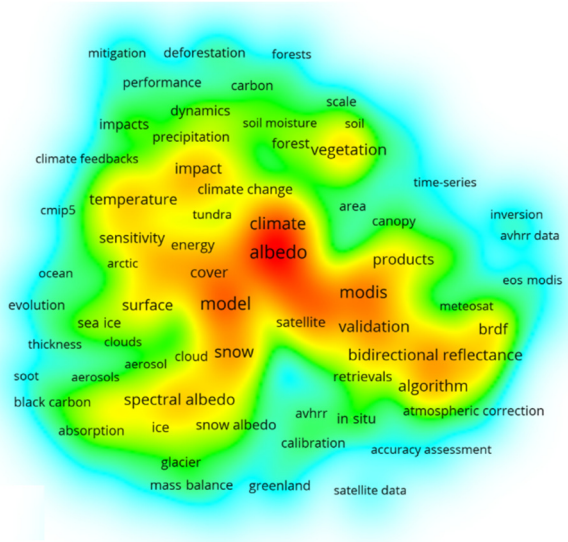

Figure 5. Density plot of keywords. Colouring from red to blue indicates decreasing frequency.

The statistics show that surface albedo has been studied for decades, and attention to the subject has increased, especially since 2008. Studies of various land types have been conducted, as shown in Figures 4 and 5, and the high use of the term "climate" indicates its close relationship to surface albedo. Many albedo management strategies have also been proposed in recent years [20], which may provide an important solution for climate mitigation.

3. Variance Characteristics of Surface Albedo for Essential Land Types and Scales

Surface albedo generally varies by land cover type for natural (e.g., wildwood) and artificial surfaces (e.g., buildings) [70,71] and is also sensitive to various factors besides atmospheric [72,73] and cloud [74] conditions, such as soil–vegetation [66,67,75,76], snow [77–79] BRDF characteristics, topography [80], diurnal asymmetry [81] and spatial resolution [82]. Some studies also focus on surface albedo across mixed land covers, special objects and hotspot regions.

3.1. Albedo Variances for Typical Land Types

3.1.1. Soil Albedo

Soil albedo is generally used as the background value of scenarios and varies with various factors, such as soil surface irregularities, wetness, soil colour, the SZA, and biochar.

For tillage soil, there is a positive correlation between surface albedo and the SZA, while a negative relationship is observed with an increase in soil roughness and wetness [83]. Specifically, highly rough soils show stable surface albedos as the SZA increases, while the smooth soil surfaces show a gradual increase in albedo. Therefore, soil roughness can act as an indicator of the diurnal variation in soil albedo [84]. Meanwhile, soil albedo is more sensitive to surface roughness under dry conditions than wet soil. In addition, soil moisture has been used to tune soil colour mapping and albedo [85], and deep soil moisture also shows a link to decreases in bare soil and canopy albedos [86]. With an increasing mass of soil accumulated salt from non-saline conditions, soil albedo can reach as high as 0.3 [87]. Moss and biocrusts significantly reduce (43.4%) bare soil albedo due to the increased darkness (43.7%), roughness (90.4%) and moisture (20.7%) of the biocrust layer [88]. Biochar application shows decreased soil albedo [89], which results in a reduction of its overall climate mitigation benefit in production, but which shows a non-negligible advantage for soil amelioration [90,91]. Spectral albedos of desert surfaces (i.e., Gobi and sand dunes) in China were measured at spectral ranges of 0.35 to 2.5 μm in the spring and autumn [92], and lower (0.05–0.11), obviously higher (0.20–0.30), and maximum values (0.37–0.49), and more variability in surface albedos at UV wavelengths, approximately 0.6 μm, around 1.8–2.2 μm, and Gobi surfaces were found, respectively.

3.1.2. Vegetation Albedo

The change in vegetation canopy albedo has essential interactions with the carbon trade-off [93], atmospheric nitrogen deposition and other environmental dynamics (e.g., temperature and precipitation) [69,94], especially for forests. Forest canopy albedo mainly varies with species (e.g., evergreen needleleaf forests, evergreen broadleaf forests, deciduous needleleaf forests, deciduous broadleaf forests, and mixed forests) [69,95], greenness [96], forest structure (e.g., forest density, the leaf area index (LAI), and fractional vegetation cover (FVC)) [97,98], stand age [95,99] and disturbance type (e.g., harvest and fire) [95]. Broadleaf-dominated species usually present higher albedo levels than conifer-dominated stands, and these values are more significant under snow-covered conditions [95]. Moreover, forest structure may modulate albedo in most sub-biomes, and there is always a positive albedo response to the LAI and a negative response to the FVC, except for deciduous broadleaf forests in Mediterranean and temperate regions [97]. Notably, leaf structure and biophysical parameters present significant effects on canopy albedo, such as leaf glossiness and/or canopy morphological traits [100] and foliage nitrogen concentration for temperate and boreal forests [94,101]. In addition, albedos of forest fine structures have also been investigated, such as the vertical albedo profile [102] and coniferous needle and shoot albedo [103].

Similarly, canopy albedos for various vegetation types in addition to forests (e.g., shrubs, crops and grass) also change with species [96]. Given that these non-forest vegetation types always have considerable intra- and interannual variations, their canopy albedo variations with spatial (regional), temporal (within the growing season), and spectral (visible, near-infrared, and shortwave) characteristics are more complex than those of forests [104]. Numerous studies have focused on crop albedo in agricultural fields [105], and biochar application to Mediterranean agricultural landscapes may reduce climate mitigation in the production of biochar due to reduced albedo [90]. In particular, different albedo variances were found among biofuel crops, such as corn, switchgrass and miscanthus in American agroecological zones [106]. In addition, shrubs in tundra ecosystems of the terrestrial cryosphere can also reduce winter albedo [107], and vegetation canopy albedo responds in opposite ways to soil moisture conditions, such as those of soil [86,108,109]. The impact of flowers on canopy albedo has also been investigated [110].

3.1.3. Snow, Ice and Water Albedos

Studies on snow albedo mainly focus on snow surfaces at a large scale at the north pole [107], the south pole [68] and alpine regions, and both pure [65] and contaminated

snow [111] have been investigated. Similar to vegetation, a series of snow physical parameters also show a significant influence on surface albedo [78,112], such as snow type [113], density [114], snow grain properties [18], snow depth, the SZA [112], roughness [115] and impurities [78]. Impurities can generally lead to a reduction in snow albedo [78,116,117], including light-absorbing particles of black carbon [18,118] and soot [64]. In addition, microscopic plants of algae [116] and tundra [107] can also reduce surface albedo in snow-covered areas.

Similar to those focused on snow, studies on ice albedo also focus on sea ice in the Arctic [119,120] and Antarctica [121]. In particular, the Kangerlussuaq transect (K-transect, Greenland ice sheet) has attracted much attention in recent years [122–126]. Moreover, ice albedo changes with a series of physical properties, such as ice type [113,127], concentration [121], roughness (e.g., weathering crust) [115,126], melt-pond depth and ice thickness [128]. In addition, impurities are another essential contributing factor. For example, salt precipitation can lead to an increase in ice albedo [129]. However, lower ice albedo is observed when ice is contaminated with many impurities, such as algae [123,126] and even algal blooms [18], soot [64], ashfall [130], Saharan dust and black carbon [131], and fire-induced aerosols [132].

In terms of water, many studies have focused on ocean surfaces that represent approximately 70% of the Earth's surface [133,134]. Ocean breaking waves [135] and ship wakes [136] can increase ocean albedo, and ocean water albedo has been calculated as a function of sun glint, whitecaps, and water-leaving reflectance [133]. Generally, the water surface presents a lower albedo than the surrounding terrestrial landscape [137]. In addition, water albedos at smaller scales are also investigated. For example, saline lake albedo increases with salt concentration [138]. For low-gradient, non-white water (flatwater) streams, the solar elevation angle, suspended sediment concentration, aeration and proportion of diffuse to direct solar radiation can enhance surface albedo from 0.025 to 0.33 [139].

Snow, ice and water can be interchangeable across seasons, which leads to varying albedos. For example, the albedo of Arctic sea ice varies during melting and refreezing periods [17,71], and impurity-induced albedo reduction of snow and glacier has enhanced glacier melt in the Tibetan Plateau [117] and the Alps [131]. Similarly, known drivers of algal blooms and cryoconite always lead to albedo reduction on ice sheets, glaciers, and snowfields [26], and microbial dark sediments also reduce the albedo of Greenland ice sheet supraglacial streams and lead to melting [125].

3.1.4. Urban Albedo

Urban albedo closely impacts UHIs and causes a series of living environmental problems [25,59], and various countermeasures have been proposed. Urban albedo varies with complex urban morphologies (e.g., block shapes, plan density, facade density, building height, and layout orientation) and other factors (e.g., latitude, time and sky-view factors) [140], and the average urban albedo is the lowest for a medium-density city with high-rise buildings presenting greater building height differences [141]. It seems to be an effective solution to increase urban albedo using retroreflective materials (RRMs) (e.g., glazed facades), which can offset anthropogenic heat emissions in residential areas [142,143]. In addition, roof albedo has attracted much attention, and analysis results show roof albedo changes based on materials (e.g., membrane, asphalt shingle, roofing aggregate and tile materials) [144]. Notably, roof membrane albedo plays a significant role in reducing heat in warmer months [145]. Moreover, pavement is another essential element in urban regions, and road albedo varies with the type [146] and ageing [147] of materials.

3.2. Albedo Variances for Mixed Land Types

Natural surfaces are always composed of mixtures of multiple land types rather than a single type. Surface albedos of the 16 International Geosphere-Biosphere Program (IGBP) ecosystem classes accompanied by snow have been investigated [70], especially

for forests [148,149], and an obvious increase in surface albedo has been observed in snow-covered areas due to their high albedo magnitude. Mixed forest albedo varies with stand age, canopy height, tree species composition and FVC [148,149]. Moss and biocrusts growing on soil significantly decrease overall soil albedo due to increased darkness [88], and a similar result is found in Greenland ice sheet supraglacial streams due to microbial dark sediments [125]. In addition, urban areas always contain soil–vegetation plots and various artificial elements (e.g., blocks, street canyons, and pavement), which present complex albedo variances [25,140,146].

3.3. Albedo Variances for Special Objects

Surface albedos of some special objects have also been noted. Within geomorphic circles, rocks with low albedos usually present higher levels of radiative warming than those with high albedos when their temperatures are no more than the surrounding air temperature. Nevertheless, as the rock temperature exceeds that of the surrounding air, their temperature variances show little difference for both dark and light rocks [150]. The impact of flower albedo on soil microclimates was also compared to the effect for vegetation without flowers [110]. Albedos of special artificial materials have also attracted much attention. In agriculture, widely used greenhouse cladding materials (e.g., commercial polymer films) offer a potential means to increase the surface albedo of the local environment, which can subsequently affect the local thermal environment [151]. Additionally, the albedos of daily necessities have also been investigated, such as those of clothing and carpets [152].

3.4. Discussion of Albedo Variances Characteristics

Numerous studies focus on well-known landscapes and regions worldwide as well as on the globe as a whole. First, the cryosphere, which is covered by perennial ice and snow with high albedo, has attracted much attention, including the Arctic and Antarctic, and high-altitude areas, such as the Asian water tower (i.e., Tibetan Plateau) and the Alps. In terms of vegetation regions, temperate and boreal forests and Mediterranean agricultural landscapes have received widespread attention. Deserts and urban landscapes have also been areas of concern. Analysis shows that surface albedo for typical land types generally varies with some common factors, such as surface structure, moisture, impurity contamination, surface inhomogeneity and roughness, surface density, SZA, and topography. In particular, snow- and ice-covered areas with high albedos have attracted much attention, because a significant change in albedo can be seen during the formation and melting periods of snow and ice. Moreover, increasing attention on special materials shows a trend in finer terrestrial monitoring.

Therefore, a surface albedo dataset with high spatiotemporal resolution and accuracy is demanded for an elaborate Earth survey. First, these typical variance characteristics summarized in this study are promising to be used as prior knowledge for an accurate estimation. In addition, with rapid development in the spatiotemporal resolution of satellite observations and remote sensing from airborne observations, such as research aircraft [153] and unmanned aerial vehicles (UAVs) [154], albedo variances at multiple scales can be investigated and compared.

4. Climate Feedback and Management Strategy for Surface Albedo

Surface albedo plays an essential role in understanding and controlling climate change. Various surface albedo datasets have been widely used to survey slow climate change, such as those for land degradation [155], rapid surface dynamics [15] and extreme disaster events, such as forest fires [156]. These variances in surface albedo have a significant effect on the carbon trade-off [29,157], and many management strategies have been implemented to mitigate greenhouse effects, such as afforestation [158] and the application of high-albedo materials for pavement and roofs in urban areas [159].

4.1. Monitoring Short-to-Long-Term Albedo Change and Climate Effects

4.1.1. Relationships between Surface Albedo Variance and Climate Feedback

Soil and vegetation are always studied together due to their closely dependent relationship. Although higher surface albedo was observed for desertification soil after removing vegetation due to overgrazing [160], denuded surfaces show positive climate feedback at higher temperatures than vegetated surfaces due to the thermal effect of soil [161]. Surface albedo shows the potential to identify arid ecosystems considering its abrupt and discontinuous increase with increased aridity [162,163]. There remains a close link between forest canopy albedo and environmental conditions (e.g., atmospheric nitrogen deposition, temperature and precipitation); therefore, it is important to elucidate the ecological mechanisms involved [69]. For temperate and boreal forests, both CO_2 uptake capacity and canopy nitrogen concentration are strongly and positively correlated with shortwave surface albedo [94]. A reduction in surface albedo was observed due to burn scars, and biomass burning aerosols showed positive direct radiative forcing close to 0.1 W/m^2 [164]. Liana-specific optical traits from thinner leaves with lower pigment concentrations show high efficiency in light interception, which can increase tropical forest albedo by 14% in the shortwave and reduce tree (−19%) and ecosystem (−7%) gross primary productivity (GPP), despite a significant increase in liana GPP (+27%) [165]. The climate effects of agricultural biofuel albedo with CO_2 and other greenhouse gas emissions have been investigated by life cycle assessment (LCA), which shows a small cooling effect (e.g., corn ethanol, −1.8 g CO_2 equivalent (CO_2-eq) for a mega-Joule (MJ) of corn ethanol) and a stronger (e.g., switchgrass ethanol, 12.1 g CO_2-eq) and less warming effect (e.g., miscanthus ethanol, 2.7 g CO_2-eq) [106]. Flower albedo can affect soil microclimates, and sunflower plots with abundant flowers were found to lead to warmer (up to 1.2 °C) and drier soils and increased plant water stress compared to plots with flowers removed [110].

Similarly, snow, ice and water are also strongly associated with each other, which can be interconverted along with changes in temperature and weather [17]. The extent of snow cover and sea ice in the Northern Hemisphere has declined since 1979 with a declined cooling effect of 0.45 W/m^2, coincident with hemispheric warming and indicative of a positive surface albedo feedback effect of surface albedo on climate as well as the total impact of the cryosphere [166]. In particular, the high albedos of snow and ice surfaces show a large effect on radiative forcing. Snowfall-induced high albedo in postfire forest areas during spring forest recovery shows large variations (e.g., >0.6) [167] and presents a predominantly negative radiative forcing [156,168], and the reduction in snow has led to an increase in Swiss spring temperatures by approximately 3–7% during 1961–2011 [169]. On a global scale, snow albedo shows a small climate feedback value of approximately 7% of that of the water vapour impact, while the peak value of snow albedo greatly affects warming during the spring due to its important driving role in regional climate change [27]. Snow and ice albedos are closely related to the mass change (also called mass balance) of snow and ice over these surfaces (e.g., snow water equivalent), which have been investigated over snowpack [170] and five glaciers in the Canadian Arctic [171] in the melt season. Specifically, the upper site of an Alps glacier has mainly experienced positive mass balances with continuously buried impurity layers over the period 1914–2014, whereas negative mass balances appeared with impurity-induced albedo reduction and increased melt at a lower site [131]. Surface melt and subsequent snow air depletion can ultimately lead to the disintegration of ice shelves and accelerate sea-level rise, and foehn winds enhance melting near the grounding line, leading to the disintegration of the most northerly ice shelves in the Antarctic Peninsula [172]. The melting of relatively thin Arctic sea ice pack was monitored in the summer [31], and reportedly, Arctic sea ice has shrunk substantially over recent decades [32]. Impurity (e.g., black carbon)-induced snow albedo reduction has greatly enhanced glacier melting on the Tibetan Plateau by approximately 15% during 2001–2018 [117], and forest fire-generated aerosols have also reduced glacier albedo by 4–81% in a 20-year record (2000 to 2019) of MODIS, leading to an increase in air temperature [132]. Continental-scale snow albedo anomalies in the meteorological activities

of wintertime Arctic oscillation were observed [173]. A small increase in precipitation in interior Antarctica can increase snow albedo by 0.4% on average during the 21st century based on simulations, which has shown an inhibition of positive SAF induced by global warming [174]. Substantial Antarctic sea ice losses from 2016–2018 reduced its negative climate feedback by an increase trend of $+0.26 \pm 0.15$ W/m^2 [175].

In addition, surface albedo changes when natural disasters occur. Climate warming and drying intensify the fire dynamics of forests (e.g., boreal forests), which leads to a shift in vegetation composition [176]. Nevertheless, studies on desert dust and biomass burning aerosols can exhibit dramatic shifts in radiative forcing at the TOA from cooling to warming at surface albedos of below 0.5 to above 0.75 [72]. During the 2003 European heat wave, a significant total negative shortwave radiative forcing (-10 W/m^2) was observed, especially over cropland areas, while a small effect (-1 W/m^2) was observed at the subcontinental scale [109]. Altered albedo dominates the radiative forcing changes in a subtropical forest following an extreme snow event [177]. Based on the analysis of a historical dataset of mountain pine beetle outbreaks in North America over a 60-year period, albedo increased, and change in annual albedo (0.06 ± 0.006 W/m^2) and negative radiative forcing (-0.8 ± 0.1 W/m^2) first reached its peak after 14–20 years and then recovered to preoutbreak levels within 30–40 years [178]. The desert shows sharp reductions in albedo to less than 0.2 when the surface is flooded [179].

Surface albedo can also be used for the interpretation of natural geographic processes and phenomena. For example, surface albedo data can aid in more accurately extracting the zenith light intensity of atmospheric emissions at night (i.e., auroral), which are always contaminated by backscattered light from the ground or clouds below the emission layer for satellite observations [180]. In addition, surface albedo impacts artificial night sky brightness at the zenith along with land types and seasons [181].

4.1.2. Albedo Variances Induced by Anthropogenic Land Use

Recently, increasing attention has been dedicated to human-induced albedo variances, and cultivation and urbanization are considered the two main factors involved [182].

For some deforested areas of the Amazon, secondary vegetation has been the dominant land cover with similar albedo levels as those of primary forests [183]. As an important source of transportation biofuel, increased forest harvesting was adopted with higher albedo and induced varying radiative forcing over time [184]. To achieve ecological goals, such as water and soil conservation and sand prevention, artificial afforestation has been widely implemented worldwide and can significantly increase carbon storage by absorbing atmospheric carbon dioxide and thus decreasing radiative forcing to cool the Earth [158]. However, surface changes from more reflective pasture to relatively less reflective forest cover can lead to a positive radiative forcing [158,185], and an overall decrease in the benefits from increased carbon storage by 17–24% was found in New Zealand [158]. In particular, the positive forcing arising from surface change from winter snow to forest in high-latitude regions may even offset the negative forcing from carbon sequestration [43,60], and an empirically-based projection made in Norway also suggests that the positive climate feedback of high-latitude and high-elevation expanding forests with seasonal snow cover exceeds that of afforestation at lower elevations in the 21st century [43]. High-albedo soils denuded by overgrazing appear much brighter and cooler than regions covered by natural vegetation under sunlit conditions, which results in a thermal depression effect and can further lead to regional climatic desertification [160]. Therefore, reindeer summer grazing greatly decreases shrub height, abundance and total biomass in pastures, which present increasing albedo and eventually delay snowmelt [186]. In terms of agriculture, anthropogenic vegetation changes have caused relatively weak global mean radiative forcing (-0.09 W/m^2) from preagricultural times to the present, but regional radiative forcing is strong in certain regions and may have resulted in regional climate changes [187]. The significant transformation from forest to cropland in China between 850 and 2015 was investigated using the historical land-use harmonization dataset and albedo look-up

maps, which shows an annual-mean increase (i.e., 0.00110) in land surface albedo and brings a slight negative radiative forcing of -0.09 ± 0.04 W/m^2 [188]. A study shows that present land-use transitions over China bring cooler summers and winters accompanied by reduced diurnal temperature ranges, and region-oriented parameterization should be applied to consider the heterogeneous biophysical effects of vegetation in different climate zones [189].

Urban construction is a major process in terms of human activity, which results in a totally slower increase in surface albedo due to transitions from canopy covers to darker impervious covers (e.g., roof and pavement) [190,191]. Thus, UHIs were first discovered in the early 1800s, which emerges as the source of many urban environmental problems and exacerbates the living environment in cities, and reflective materials are expected to help tackle these challenges [25]. The LCA of urban roofs shows that high-albedo materials can effectively mitigate UHIs [192]. Moreover, the LCA of pavement albedo has a varying impact on the carbon budget along with materials, where Portland cement concrete pavement reduces CO_2-equivalent emissions by 9.2%, and an increase of 19.1% was observed for hot mixture asphalt pavement [193]. Computational fluid dynamics (CFD) analyses of asphalt and concrete pavements under the same ambient conditions show that asphalt surface temperatures are consistently higher, and surface temperatures decrease with increasing surface albedo and thermal inertia values for the two materials, especially for surface albedo [194]. Although a high-albedo street canyon can mitigate the UHI effect, the corresponding mean radiant temperature can increase pedestrian heat stress [195]. In addition, urban-industrial aerosol haze can exhibit dramatic shifts in radiative forcing at the TOA from cooling to warming with changes in surface albedo [72].

4.1.3. Application in Ecology and Climate Simulations

Land surface albedo datasets play an essential role in the evaluation and tuning of most regional and global energy budgets, climates, ecology and biogeochemical models [2]. For example, precise ocean albedo data can significantly reduce the biases of ocean–atmosphere coupled tropical-channel models [196] and Earth system models over tropical oceans [134].

First, surface albedo plays a key role in surface energy and radiation budget models [4]. The impact of ice/snow albedo has attracted particular attention. Based on an energy balance model (EBM) of the Earth's climate, the change in the winter snow line in the middle-latitude plateau of Northern Hemisphere topography can lead to an enhancement of positive SAF [16]. The National Center for Atmospheric Research Community Climate Model is used to calculate the increase in solar energy that would be absorbed by the Earth–atmosphere system if all sea ice on the planet were to melt, which presents an upper limit compared to the direct radiative forcing of greenhouse gases, such as atmospheric carbon dioxide [197]. Snow albedo is used to describe the seasonal cycle of snow hydrology [112]. By coupling an atmospheric general circulation model with a sea ice–slab ocean model, the extreme climate of full Earth glaciation is simulated by different surface albedos in conjunction with CO_2, orography and oceanic heat transport [198]. Based on an Earth system model, high snow albedo can lead to excessive ice build-up during glacial times [199]. In early stages, an "almost trivial" climate system of geometrical dimension zero was developed and was used to analyse the impact of ice albedo on climate feedback, including three main climate states of interglacial, deep freeze and desert heat [200]. Notably, coupled climate Community Climate System Model v3 (CCSM3) [201] and v4 (CCSM4) [202] were used to simulate and explain the famous Arctic amplification phenomenon, where a substantial reduction in sea ice in the Arctic has been observed at nearly double the warming rate of the global average. Dynamic simulations based on the diurnal EBM implemented in the parallel ice sheet model (PISM) show that SIAF is an essential contributor to the mass loss of the Greenland ice sheet under future warming, which further contributes a large amount to future sea-level rise [203]. The terrestrial cryosphere is mainly composed of snow, glaciers and ice, and covers approximately one-fifth of the Earth, and the ongoing

and predicted impacts of cryosphere loss may lead to the disappearance of entire biomes and crises of water availability.

In addition, vegetation and urban albedos also have essential impacts on climate change. A two-dimensional cellular automaton Daisyworld was developed to study interactions between environmental conditions (e.g., background albedo and temperature) and organism growth [204]. Forests often suffer from insect plagues, and modelling of mountain pine beetle outbreaks over 240 years shows a reduction in merchantable biomass and an increase in surface albedo; however, these outbreaks may have a much smaller impact on global temperatures over the coming decades and centuries than a single month of global anthropogenic CO_2 emissions from fossil fuel combustion and cement production [205]. In addition, previous findings highlight the strong sensitivity of summer monsoon circulation and rainfall to surface albedo in an ocean–atmosphere coupled model [196]. Interaction between wind and surface albedo was modelled in low dust emitting regions of stony deserts by using the Weather Research and Forecasting (WRF) model; fine-grained sediments and low-albedo gravel-mantled surfaces can alter surficial thermal properties and increase near-surface winds by up to 25%, and wind erosion results in faster winds regionally [206]. High-albedo materials may be used widely in urban areas, particularly in warm and hot climates, and a modelling study shows their ability to achieve higher air quality with a net effect of reducing ozone concentrations [207]. A three-dimensional numerical model (the Model for Urban Surface Temperature (MUST)) was used to investigate the impact of urban geometry on average urban albedo and street surface temperature, where the average sky-view factor plays an essential role [141]. A numerical model was used to evaluate the impact of street canyons on subsequent pedestrian heat stress using the mean radiant temperature [141], and the optimal combinations of urban albedo and green covering were determined to improve the urban microclimate (e.g., outdoor air temperature and mean radiant temperature) based on environmental analysis model ENVI-met [208,209]. Based on a WRF model, high-albedo urban materials can mitigate the UHI effect but worsen the outdoor thermal sensation [210].

In addition, large-scale climate change has been associated with surface albedo based on a series of circulation and forecast models in global climate forecasts [211,212] and regional weather forecasts [213]. Near real-time surface albedo has been used to improve the Noah land surface model [212]. Although carbon sequestration or modern biomass plantations can mitigate the greenhouse climate by 2100 according to integrated assessment model IMAGE 2.2, the subsequent reduction in surface albedo can increase surface temperature and offset climate contributions [214]. According to simulations by IPCC AR5 Coupled Model Intercomparison Project Phase 5 (CMIP5) for the past 150 years using the climate model and emissions from preindustrial times to the present day [73], aerosols show a small positive radiative forcing induced by their surface albedos (+0.016 W/m^2) and would lead to ten times larger positive TOA radiative forcing, although the overall effect on solar radiation and clouds is most certainly negative (-0.6 W/m^2). Emergent constraints are proposed to reduce intermodel variability in projections of climate change based on CMIP6 [215], which occurs each year as snow and sea ice retreat from their seasonal maxima and which is strongly correlated with future surface albedo feedback in modern-day analogues. Based on general circulation model ECHAM5-JSBACH, the dynamics of vegetation albedo and background soil albedo have shown an improvement in the frequency and persistence of precipitation anomalies in the Sahel region, respectively [216]. In addition, cloud-compensated hemispheric asymmetries in clear-sky albedo show that hemispheric albedo asymmetries have induced a series of climate changes by coupling ECHAM6 to a slab ocean model [217]. Eleven Earth system models are used to investigate climate effects by maintaining net TOA radiation balance with an imposed forcing of an abrupt quadrupling of the CO_2 concentration and an instantaneous increase in ocean albedo, and opposing trends are observed for air temperature over the land surface (increase by 1.14 °C on average) and most of the ocean (decrease) [19]. These results reinforce previous findings that keeping TOA net radiation constant is not sufficient for pre-

venting changes in global mean temperature. In particular, surface albedo is also necessary to model climate variances in past periods, such as the impact of surface albedo on climate variations in the Phanerozoic [218], Sahel/Sahara precipitation in the mid-Holocene [219], the "Snowball Earth" hypothesis of the Neoproterozoic glacial episodes [220], the early Archean climate [221] and the Pliocene Arctic climate [222].

4.2. Economic Cost and Management Strategy for Surface Albedo

Based on the relationships between surface albedo and ecology as well as economic benefits, various management strategies for surface albedo have been proposed. In the Albedo, Building green, Control of global warming and Desertification (ABCD) project conducted in 2012 in Italy, the installation of highly reflective surfaces was demonstrated to be an effective means to tackle global warming by achieving a significant offset of CO_2 equivalents [20]. A simulation shows that albedo modification produces substantial near-term reductions in the rate of Greenland ice sheet-driven sea-level rise, while continued sea-level rise contributions persist for decades to centuries after temperature stabilization and temperature drawdown begin [122]. To implement land-based climate mitigation, non-CO_2 forcing agents are often converted into "physical" CO_2 equivalents [29,93], and social-cost-based CO_2 equivalents for surface albedo-induced forcing are also proposed as stock equivalents to assist economic analysis [157].

Numerous studies have focused on soil and vegetation albedo management, especially for forests. The magnitude of the carbon offset potential due to changes in surface albedo has been simulated based on climate models over a 100-year management period, which has important implications for forest management methods to mitigate climate change in light of this additional biophysical criterion [184]. Four methodologies are utilized to calculate shadow prices for forest albedo radiative forcing, which are then input to an ecological and economic forest model to determine optimal rotation periods [223]. Carbon-equivalent metrics for forest albedo changes have been proposed [93], and the cost of forest climate mitigation associated with both carbon sequestration and albedo change seems to be more efficient and less intrusive than the traditional policy that merely considers carbon sinks [224]. Afforestation is taken as an essential climate mitigation option incentivized by a globally uniform reward for carbon uptake in the terrestrial biosphere, but it could lead to food price hikes through land competition [185]. A market-level model has been explored with socially optimal carbon and albedo pricing and characterizes optimal land allocation and harvests by considering both climate benefits and economic welfare [225]. Most biogeophysical forcings (e.g., surface albedo-induced radiative forcing) are rarely included in climate policies for forestry and other land management projects due to quantification challenges, and more coordinated research among terrestrial ecologists, resource managers, and coupled climate modellers is needed to corroborate and validate metrics at multiple scales [24].

Crop management is another essential albedo strategy that involves changing agricultural practices. A "biogeoengineering" approach was proposed to mitigate surface warming, whereby specific crop varieties (e.g., specific leaf glossiness and canopy morphological traits) are chosen to maximize canopy albedo [100,226]. Agricultural lands span 15% of the global ice-free terrestrial surface and provide an immense and near-term opportunity to address climate change, food, and water security challenges. The breeding of new cultivars is computationally informed based on different canopy structural traits to increase productivity, water use efficiency, and surface albedo to offset greenhouse gas warming [227]. Reducing or suppressing tillage (no-till) shows the potential to sequester carbon in soils and albedo-induced cooling with higher albedo from soil than crops, which opens new avenues for climate engineering measures targeting regional hot extreme events [228]. The incorporation of charcoal produced by biomass pyrolysis (biochar) in agricultural soils is a potentially sustainable strategy in soil amelioration, while large-scale biochar application with low albedo may result in some side effects, such as warming effects [90,91]. Different from the traditional view that wood fuels are carbon neutral,

similar to other bioenergy sources, and considering the offset of CO_2 sequestration by biomass regrowth to CO_2 release, quantified studies over a 100-year time horizon show that bioenergy from slow-growing forests usually has a greater global warming potential (GWP) than fossil oil and gas, while the results associated with coal are condition-dependent [229]. Biofuel crops are considered useful climate benefits due to land conversions, and the LCA analysis shows a small cooling effect (e.g., corn ethanol, −1.8 g CO_2-eq) and a stronger (e.g., switchgrass ethanol, 12.1 g CO_2-eq) and smaller warming effect (e.g., miscanthus ethanol, 2.7 g CO_2-eq) [106]. However, a different conclusion was found that an albedo-induced climate mitigation for perennial (e.g., switchgrass) but not annual (e.g., corn) bioenergy crops shows a much greater cooling effect [230].

Moreover, many management methods have been proposed to control the surface albedo of water cycle process factors for snow, ice and water to mitigate global climate warming. Vehicle emissions in the surroundings of ski resorts can reduce snow whiteness and accelerate snowmelt, which affects attractiveness for visitors; therefore, traffic restrictions may allow for more stable snowpack and regional climate conditions [231]. The positive SIAF in the Arctic has amplified warming, which has driven further melting, and thus, reducing model errors in the current seasonal climate feedback and ice thickness can narrow its spread under climate change [32]. The increasing global temperature not only results in the melting of the Greenland ice sheet but also in albedo loss and in turn reduces the strength of SAF and increases the social cost of carbon [232]. For low-albedo water, one feasible method is to brighten the surface of the ocean by increasing the albedo and areal extent of bubbles in existing shipping wakes, and simulations show that the addition of surfactant is required to extend the wake lifetime from minutes to days and months to achieve a significant negative global radiative forcing [136]. Geoengineering on the ocean surface albedo scheme was performed based on a series of Earth system models and shows that the maintenance of the TOA net radiation constant is not sufficient for preventing changes in global mean temperature [19]. Lower albedo in the water of hydropower reservoirs than in terrestrial landscapes results in a positive radiative forcing and offsets some of the negative radiative forcing of hydroelectricity generation; in the future, hydropower plants need to minimize the albedo penalty to make a meaningful contribution towards limiting global warming [137].

In city management, albedo mitigation strategies are widely used, and square urban grids show more potential to reduce the average hourly temperature by using fewer mitigated points [233]. An LCA of different roofs shows that high surface albedo plays a crucial role in offsetting radiative forcings with a decrease in CO_2 equivalents and mitigation of the UHI; a highly reflective roof can also save annual cooling energy use relative to a low-albedo roof [234]. A new type of RRM has been developed as a building coating to help counter UHIs, and building surfaces with RRMs are more effective than other materials with diffuse or mirror reflective characteristics [143]. However, precautions need to be exercised by city planners and policy makers pursuing the large-scale deployment of reflective materials without a sufficient understanding of their environmental impacts, especially on regional hydroclimates, and the optimal strategy for UHIs needs to be determined on a city-by-city basis rather than with a "one-solution-fits-all" approach [25]. The use of high-albedo materials further worsens thermal sensation due to further decreased wind speed in addition to its considerable benefits in terms of temperature and energy savings in heat waves; therefore, its application requires a careful evaluation of benefits and side effects [109,210]. Similarly, pavement materials with high surface albedo have been investigated, where Portland cement concrete slabs show higher surface albedo and lower internal temperatures than asphalt mixture slabs [146]. Moreover, the implementation of urban greenery is a widely adopted mitigation strategy to reduce ambient and surface temperatures, which can then mitigate the UHI effect [235].

In addition, some industry management is also associated with surface albedo. Surface albedo can affect the performance of solar cells (e.g., short-circuit current density, open-circuit voltage, fill factor and output power) [236], and improvements in efficiency of over

50% [237] and 30% [238] have been reported. Specifically, a new solar cell design based on bifacial heterojunction back contact shows an improvement in maximum power density by 8% at 20% albedo compared to the monofacial condition [239]. A simulation of shadow losses of direct normal, diffuse solar radiation and albedo for a very large number of trackers used in photovoltaic systems was calculated, which provides guidance for the usage of these trackers [240]. The UV damage from the combinations of 35 types of grounding materials and 4 types of common photovoltaic backsheets was evaluated theoretically, and it was found that a more accurate evaluation can be obtained by considering the spectral albedo and long-term reliability of photovoltaic systems [241]. The anthropogenic increase in aerosol concentrations since preindustrial times shows a small positive radiative forcing (+0.016 W/m^2) induced by the reduction in surface albedos and a significantly positive TOA radiative forcing (-0.6 W/m^2) [241]; the most responsible sectors are pointed out, including the transportation sector in the United States, agricultural burning and transportation in Europe, and the domestic emission sector in Asia. These evaluations can help promote the division of climate responsibility and provide solutions. Climate has been recognized as having direct and indirect impacts on society and the economy, both in the long term and in daily life; therefore, multiagency collaborations are in high demand in future work [242].

4.3. Discussion of Albedo-Induced Climate Feedback and Albedo Management Methods

Among numerous studies on the relationship between albedo and climate, some inconsistencies and novel points must be noted. First, although the increase in surface albedo has widely been considered to be a clear and effective solution to mitigate global warming, complex climate mechanisms always lead to varying and even opposing conclusions at different spatiotemporal scales [109,187]. In particular, the climate effect of agricultural biofuels changes with albedo, and different findings have been obtained, including warming [106] and cooling effects [230]. Meanwhile, albedo-induced side effects have been emphasized in several studies when evaluating climate effect, such as the impact of biochar and highly reflective roof materials on soil amelioration [90,91] and thermal comfort of pedestrians [109,210], respectively. In addition, the traditional view holds that wood fuels are green energy resources and promising replacements for fossil fuels, while quantified studies show that wood fuels may lead to a stronger warming effect than fossil fuels [229]. These inconsistent and even controversial analyses conducted at multiple spatiotemporal scales and simulated from many climate models may be ascribed to scale differences and uncertainties in the surface albedo dataset and climate evaluation models. Therefore, a suitable spatiotemporal scale needs to be investigated for different subjects, and improvements and selections are needed for surface albedo products and evaluation models [29] to achieve greater accuracy and consistent conclusions.

Despite these inconsistencies, the sensitive surface albedo-induced climate feedback demonstrated by numerous studies provides confidence in climate indication, and subsequent albedo management strategies provide practical suggestions on achieving CO_2 emission peak and carbon-neutral goals for multiple countries. Global warming has increased the onset frequency and intensity of a series of extreme climate events [8], which directly affect human survival and urgently need to be resolved worldwide. In terms of disaster prevention and mitigation, previous architectures have mainly focused on the albedo variance characteristics of typical disasters, such as UHIs, hot extremes, forest fires, drought, and floods. Surface albedo is promising for further investigating the formation mechanisms of these disasters, accurate prediction and control measures, and other kinds of climate and meteorological events (e.g., cool extremes and hurricanes) induced by global warming. For time range selection, the long-term LCA method adopted by an increasing number of studies (e.g., decades or 100 years) is recommended to evaluate the comprehensive influence [106,184,192,193]. It should be noted that abbreviations used in this study are presented in Abbreviations part.

5. Conclusions

Global warming has increased the onset frequency and intensity of a series of extreme climate events [8], which directly affect human survival and urgently need to be resolved worldwide. As a controlling parameter in the surface energy balance, surface albedo shows to be a promising approach to climate mitigation. In this paper, we present a comprehensive review of surface albedo based on architecture analyses, focusing on its variance patterns, climate feedback and management strategies. The salient points are summarized as follows:

(1) A more specific term, "surface albedo", is recommended for inclusion in titles and keywords instead of "albedo" to avoid confusion (e.g., planetary albedo), and the high frequency of the word "climate" indicates many efforts have been made in dealing with climate problems using surface albedo data. Although many albedo management strategies have been proposed in recent years [20], their quantity and influence are still limited and need to be further developed.

(2) A significant surface albedo-induced climate feedback has been observed, and many studies focus on enhanced glacier, ice and snow melt in the Arctic and Antarctic induced by increasing global temperature, high albedo loss and albedo reduction due to impurities. However, there are some inconsistent and even controversial analyses at multiple spatiotemporal scales simulated from many climate models [109,187]. Therefore, it is necessary to investigate the suitable spatiotemporal scale for different subjects, and improvements of surface albedo product and climate models are also required for accurate climate evaluation [29].

(3) In addition, a series of effective management schemes regarding surface albedo show the potential to mitigate global warming, which provide practical suggestions for achieving CO_2 emission peaks and carbon-neutral goals worldwide. The LCA method should be used for surface albedo-induced climate feedback analysis to avoid inconsistencies in conclusions [106], and more coordinated research among terrestrial ecologists, resource managers, and coupled climate modellers is needed to support the making of climate policies [24]. Through the improvements to the spatiotemporal resolution of satellite observations and remote sensing from airborne observations, surface albedo monitoring at finer levels would help better understand environmental and climate dynamic processes as well as facilitate interventions.

Author Contributions: Conceptualization, X.Z. and Z.J.; data curation, X.Z.; formal analysis, X.Z., Z.J., C.Z., Y.T., C.W., S.L., J.G., Z.Z., S.Y., H.Z. and L.C.; methodology, X.Z. and Z.J.; funding acquisition, Z.J., X.Z. and H.Z.; writing—original draft, X.Z.; and writing—review and editing, X.Z., Z.J., Y.Q. and Q.L. All authors have read and agreed to the published version of the manuscript.

Funding: This work was supported in part by the National Natural Science Foundation of China (42090013 and 41971288), the China Postdoctoral Science Foundation under Grant 2021M690424, and the National Natural Science Foundation of China 41971306.

Data Availability Statement: All data used in this study are openly and freely available. The literature data were collected from the Web of Science core database, Thomson Reuter at https://access.clarivate.com/, accessed on 16 January 2022.

Acknowledgments: We are grateful for the careful review and valuable comments provided by the anonymous reviewers.

Conflicts of Interest: The authors declare no conflict of interest.

Abbreviations

The following abbreviations used in this study:

Abbreviations	Full Name
ABCD	Albedo, Building Green, Control of Global Warming and Desertification
AOD	Aerosol Optical Depth
BRDF	Bidirectional Reflectance Distribution Function
BSA	Black-Sky Albedo

CCSM	Community Climate System Model
CFD	Computational Fluid Dynamics
CMIP	Coupled Model Intercomparison Project
EBM	Energy Balance Model
ECV	Essential Climate Variable
FVC	Fractional Vegetation Cover
GCOS	Global Climate Observing System
GLASS	Global Land Surface Satellite
GPP	Gross Primary Productivity
GWP	Global Warming Potential
IGBP	International Geosphere-Biosphere Program
IPCC	Intergovernmental Panel on Climate Change
LAI	Leaf Area Index
LCA	Life Cycle Assessment
MODIS	Moderate Resolution Imaging Spectroradiometer
MUST	Model for Urban Surface Temperature
NIR	Near-Infrared
PISM	Parallel Ice Sheet Model
RAA	Relative Azimuth Angle
RRM	Retroreflective Materials
SAF	Snow Albedo Feedback
SDG	Sustainable Development Goals
SIAF	Sea-Ice Albedo Feedback
SSA	Single Scattering Albedo
SZA	Solar Zenith Angle
TOA	Top of Atmosphere
UAV	Unmanned Aerial Vehicle
UHI	Urban Heat Island
UV	Ultraviolet
VZA	View Zenith Angle
WMO	World Meteorological Organization
WRF	Weather Research and Forecasting
WSA	White-Sky Albedo

References

1. Dickinson, R.E. Land Surface Processes and Climate-Surface Albedos and Energy Balance. *Adv. Geophys.* **1983**, *25*, 305–353.
2. Henderson-Sellers, A.; Wilson, M.F. Surface Albedo Data for Climatic Modeling. *Rev. Geophys.* **1983**, *21*, 1743–1778. [CrossRef]
3. Dickinson, R.E. Land Processes in Climate Models. *Remote Sens. Environ.* **1995**, *51*, 27–38. [CrossRef]
4. Liang, S.; Wang, D.; He, T.; Yu, Y. Remote Sensing of Earth's Energy Budget: Synthesis and Review. *Int. J. Digit. Earth* **2019**, *12*, 737–780. [CrossRef]
5. Goodwin, P.; Katavouta, A.; Roussenov, V.M.; Foster, G.L.; Rohling, E.J.; Williams, R.G. Pathways to 1.5 Degrees C and 2 Degrees C Warming Based on Observational and Geological Constraints. *Nat. Geosci.* **2018**, *11*, 102. [CrossRef]
6. Millar, R.J.; Fuglestvedt, J.S.; Friedlingstein, P.; Rogelj, J.; Grubb, M.J.; Matthews, H.D.; Skeie, R.B.; Forster, P.M.; Frame, D.J.; Allen, A.R. Emission Budgets and Pathways Consistent with Limiting Warming to 1.5 °C. *Nat. Geosci.* **2017**, *10*, 741. [CrossRef]
7. Otto, F.E.L.; Frame, D.J.; Otto, A.; Allen, M.R. Embracing Uncertainty in Climate Change Policy. *Nat. Clim. Chang.* **2015**, *5*, 917. [CrossRef]
8. Masson-Delmotte, V.; Zhai, P.; Pirani, A.; Connors, S.L.; Péan, C.; Berger, S.; Caud, N.; Chen, Y.; Goldfarb, L.; Gomis, M.I.; et al. IPCC, 2021: Summary for Policymakers. In *Climate Change 2021: The Physical Science Basis. Contribution of Working Group I to the Sixth Assessment Report of the Intergovernmental Panel on Climate Change*; IPCC: Geneva, Switzerland, 2021; pp. 1–40.
9. Taalas, P. *The Global Observing System for Climate: Implementation Needs*; GCOS: Guayaquil, Ecuador, 2016; pp. 1–325.
10. Corner, S.P. The Sixth Major IPCC Assessment Report and its Implications: 15 September 2021. *Weather* **2022**, *77*, 70–71. [CrossRef]
11. Schaaf, C.B.; Gao, F.; Strahler, A.H.; Lucht, W.W.; Li, X.W.; Tsang, T.; Strugnell, N.C.; Zhang, X.Y.; Jin, Y.F.; Muller, J.P.; et al. First Operational BRDF, Albedo Nadir Reflectance Products from MODIS. *Remote Sens. Environ.* **2002**, *83*, 135–148. [CrossRef]
12. Liang, S.L. Narrowband to Broadband Conversions of Land Surface Albedo I Algorithms. *Remote Sens. Environ.* **2001**, *76*, 213–238. [CrossRef]
13. Qu, Y.; Liang, S.; Liu, Q.; He, T.; Liu, S.; Li, X. Mapping Surface Broadband Albedo from Satellite Observations: A Review of Literatures on Algorithms and Products. *Remote Sens.* **2015**, *7*, 990–1020. [CrossRef]

14. Liang, S.L.; Zhao, X.; Liu, S.H.; Yuan, W.P.; Cheng, X.; Xiao, Z.Q.; Zhang, X.T.; Liu, Q.; Cheng, J.; Tang, H.R.; et al. A Long-Term Global LAnd Surface Satellite (GLASS) Data-Set for Environmental Studies. *Int. J. Digit. Earth* **2013**, *6*, 5–33. [CrossRef]
15. Wang, Z.; Schaaf, C.B.; Sun, Q.; Shuai, Y.; Roman, M.O. Capturing Rapid Land Surface Dynamics with Collection V006 MODIS BRDF/NBAR/Albedo (MCD43) Products. *Remote Sens. Environ.* **2018**, *207*, 50–64. [CrossRef]
16. Birchfield, G.E.; Wertman, J. Topography, Albedo-Temperature Feedback, and Climate Sensitivity. *Science* **1983**, *219*, 284–285. [CrossRef]
17. Laine, V.; Manninen, T.; Riihela, A. High Temporal Resolution Estimations of the Arctic Sea Ice Albedo during the Melting and Refreezing Periods of the Years 2003-2011. *Remote Sens. Environ.* **2014**, *140*, 604–613. [CrossRef]
18. Wang, X.; Shi, T.; Zhang, X.; Chen, Y. An Overview of Snow Albedo Sensitivity to Black Carbon Contamination and Snow Grain Properties Based on Experimental Datasets across the Northern Hemisphere. *Curr. Pollut. Rep.* **2020**, *6*, 368–379. [CrossRef]
19. Kravitz, B.; Rasch, P.J.; Wang, H.; Robock, A.; Gabriel, C.; Boucher, O.; Cole, J.N.S.; Haywood, J.; Ji, D.; Jones, A.; et al. The Climate Effects of Increasing Ocean Albedo: An Idealized Representation of Solar Geoengineering. *Atmos. Chem. Phys.* **2018**, *18*, 13097–13113. [CrossRef]
20. Cotana, F.; Rossi, F.; Filipponi, M.; Coccia, V.; Pisello, A.L.; Bonamente, E.; Petrozzi, A.; Cavalaglio, G. Albedo Control as an Effective Strategy to Tackle Global Warming: A Case Study. *Appl. Energy* **2014**, *130*, 641–647. [CrossRef]
21. Gueymard, C.A.; Lara-Fanego, V.; Sengupta, M.; Xie, Y. Surface Albedo and Reflectance: Review of Definitions, Angular and Spectral Effects, and Intercomparison of Major Data Sources in Support of Advanced Solar Irradiance Modeling over the Americas. *Sol. Energy.* **2019**, *182*, 194–212. [CrossRef]
22. Lin, X.; Wen, J.; Tang, Y.; Ma, M.; You, D.; Dou, B.; Wu, X.; Zhu, X.; Xiao, Q.; Liu, Q. A Web-Based Land Surface Remote Sensing Products Validation System (LAPVAS): Application to Albedo Product. *Int. J. Digit. Earth* **2018**, *11*, 308–328. [CrossRef]
23. Loew, A.; Bennartz, R.; Fell, F.; Lattanzio, A.; Doutriaux-Boucher, M.; Schulz, J. A Database of Global Reference Sites to Support Validation of Satellite Surface Albedo Datasets (SAVS 1.0). *Earth Syst. Sci. Data* **2016**, *8*, 425–438. [CrossRef]
24. Bright, R.M.; Zhao, K.; Jackson, R.B.; Cherubini, F. Quantifying Surface Albedo and Other Direct Biogeophysical Climate Forcings of Forestry Activities. *Glob. Chang. Biol.* **2015**, *21*, 3246–3266. [CrossRef] [PubMed]
25. Yang, J.; Wang, Z.; Kaloush, K.E. Environmental Impacts of Reflective Materials: Is High Albedo a 'Silver Bullet' for Mitigating Urban Heat Island? *Renew. Sust. Energy Rev.* **2015**, *47*, 830–843. [CrossRef]
26. Hotaling, S.; Lutz, S.; Dial, R.J.; Anesio, A.M.; Benning, L.G.; Fountain, A.G.; Kelley, J.L.; McCutcheon, J.; Skiles, S.M.; Takeuchi, N.; et al. Biological Albedo Reduction on Ice Sheets, Glaciers, and Snowfields. *Earth-Sci. Rev.* **2021**, *220*, 103728. [CrossRef]
27. Thackeray, C.W.; Fletcher, C.G. Snow Albedo Feedback: Current Knowledge, Importance, Outstanding Issues and Future Directions. *Prog. Phys. Geogr.-Earth Environ.* **2016**, *40*, 392–408. [CrossRef]
28. Park, C.; Takeuchi, N. Unmasking Photogranulation in Decreasing Glacial Albedo and Net Autotrophic Wastewater Treatment. *Environ. Microbiol.* **2021**, *23*, 6391–6404. [CrossRef]
29. Bright, R.M.; Lund, M.T. CO_2-equivalence Metrics for Surface Albedo Change Based on the Radiative Forcing Concept: A Critical Review. *Atmos. Chem. Phys.* **2021**, *21*, 9887–9907. [CrossRef]
30. Turner, J.; Parisi, A.V. Ultraviolet Radiation Albedo and Reflectance in Review: The Influence to Ultraviolet Exposure in Occupational Settings. *Int. J. Environ. Res. Public Health* **2018**, *15*, 1507. [CrossRef]
31. Divine, D.V.; Granskog, M.A.; Hudson, S.R.; Pedersen, C.A.; Karlsen, T.I.; Divina, S.A.; Renner, A.H.H.; Gerland, S. Regional Melt-Pond Fraction and Albedo of Thin Arctic First-Year Drift Ice in Late Summer. *Cryosphere* **2015**, *9*, 255–268. [CrossRef]
32. Thackeray, C.W.; Hall, A. An Emergent Constraint on Future Arctic Sea-Ice Albedo Feedback. *Nat. Clim. Chang.* **2019**, *9*, 972. [CrossRef]
33. Nicodemus, F.E.; Richmond, J.C.; Hsia, J.J.; Ginsberg, I.W.; Limperis, T. *Geometrical Considerations and Nomenclature for Reflectance*; National Bureau of Standards: Washington, DC, USA, 1977; pp. 1–52.
34. Vermote, E.F.; Tanre, D.; Deuze, J.L.; Herman, M.; Morcette, J. Second Simulation of the Satellite Signal in the Solar Spectrum, 6S: An overview. *IEEE Trans. Geosci. Remote Sens.* **1997**, *35*, 675–686. [CrossRef]
35. Lucht, W.W.; Schaaf, C.B.; Strahler, A.H. An Algorithm for the Retrieval of Albedo from Space Using Semiempirical BRDF Models. *IEEE Trans. Geosci. Remote Sens.* **2000**, *38*, 977–998. [CrossRef]
36. He, T.; Liang, S.L.; Wang, D.D.; Cao, Y.F.; Gao, F.; Yu, Y.Y.; Feng, M. Evaluating Land Surface Albedo Estimation from Landsat MSS, TM, ETM Plus, and OLI Data Based on the Unified Direct Estimation Approach. *Remote Sens. Environ.* **2018**, *204*, 181–196. [CrossRef]
37. Zhang, X.; Jiao, Z.; Dong, Y.; He, T.; Ding, A.; Yin, S.; Zhang, H.; Cui, L.; Chang, Y.; Guo, J.; et al. Development of the Direct-Estimation Albedo Algorithm for Snow-Free Landsat TM Albedo Retrievals Using Field Flux Measurements. *IEEE Trans. Geosci. Remote Sens* **2020**, *58*, 1550–1567. [CrossRef]
38. Wang, Z.S.; Schaaf, C.B.; Strahler, A.H.; Chopping, M.J.; Roman, M.O.; Shuai, Y.M.; Woodcock, C.E.; Hollinger, D.Y.; Fitzjarrald, D.R. Evaluation of MODIS Albedo Product (MCD43A) over Grassland, Agriculture and Forest Surface Types during Dormant and Snow-Covered Periods. *Remote Sens. Environ.* **2014**, *140*, 60–77. [CrossRef]
39. He, T.; Zhang, Y.; Liang, S.; Yu, Y.; Wang, D. Developing Land Surface Directional Reflectance and Albedo Products from Geostationary GOES-R and Himawari Data: Theoretical Basis, Operational Implementation, and Validation. *Remote Sens.* **2019**, *11*, 2655. [CrossRef]

40. Pohl, C.; Istomina, L.; Tietsche, S.; Jkel, E.; Heygster, G. Broadband Albedo of Arctic Sea Ice from MERIS Optical Data. *Cryosphere* **2020**, *14*, 165–182. [CrossRef]
41. Pendergrass, A.G.; Conley, A.; Vitt, F.M. Surface and Top-of-Atmosphere Radiative Feedback Kernels for CESM-CAM5. *Earth Syst. Sci. Data* **2018**, *10*, 317–324. [CrossRef]
42. Bright, R.M.; O'Halloran, T.L. Developing a Monthly Radiative Kernel for Surface Albedo Change from Satellite Climatologies of Earth's Shortwave Radiation Budget: CACK V1.0. *Geosci. Model Dev.* **2019**, *12*, 3975–3990. [CrossRef]
43. De Wit, H.A.; Bryn, A.; Hofgaard, A.; Karstensen, J.; Kvalevag, M.M.; Peters, G.P. Climate Warming Feedback from Mountain Birch Forest Expansion: Reduced Albedo Dominates Carbon Uptake. *Glob. Chang. Biol.* **2014**, *20*, 2344–2355. [CrossRef]
44. Stephens, G.L.; O'Brien, D.; Webster, P.J.; Pilewski, P.; Kato, S.; Li, J. The Albedo of Earth. *Rev. Geophys.* **2015**, *53*, 141–163. [CrossRef]
45. Seidel, D.J.; Feingold, G.; Jacobson, A.R.; Loeb, N. Detection Limits of Albedo Changes Induced by Climate Engineering. *Nat. Clim. Chang.* **2014**, *4*, 93–98. [CrossRef]
46. Jacobson, M.Z. Global Direct Radiative Forcing Due to Multicomponent Anthropogenic and Natural Aerosols. *J. Geophys. Res.-Atmos.* **2001**, *106*, 1551–1568. [CrossRef]
47. Schwartz, S.E. Are Global Cloud Albedo and Climate Controlled by Marine-Phytoplankton. *Nature* **1988**, *336*, 441–445. [CrossRef]
48. Charlson, R.J.; Lovelock, J.E.; Andreae, M.O.; Warren, S.G. Oceanic Phytoplankton, Atmospheric Sulfur, Cloud Albedo and Climate. *Nature* **1987**, *326*, 655–661. [CrossRef]
49. Carder, K.L.; Liu, C.C.; Lee, Z.P.; English, D.C.; Patten, J.; Chen, F.R.; Ivey, J.E.; Davis, C.O. Illumination and Turbidity Effects on Observing Faceted Bottom Elements with Uniform Lambertian Albedos. *Limnol. Oceanogr.* **2003**, *48*, 355–363. [CrossRef]
50. Wu, B.; Liu, W.C.; Grumpe, A.; Woehler, C. Construction of Pixel-Level Resolution DEMs from Monocular Images by Shape and Albedo from Shading Constrained with Low-Resolution DEM. *ISPRS J. Photogramm.* **2018**, *140*, 3–19. [CrossRef]
51. Lewis, N.K.; Cook, T.A.; Wilton, K.P.; Chakrabarti, S.; France, K.; Gordon, K.D. Far-Ultraviolet Dust Albedo Measurements in the Upper Scorpius Cloud Using the Spinr Sounding Rocket Experiment. *Astrophys. J.* **2009**, *706*, 306–318. [CrossRef]
52. Luszik-Bhadra, M.; Zimbal, A.; Busch, F.; Eichelberger, A.; Engelhardt, J.; Figel, M.; Frasch, G.; Guenther, K.; Jordan, M.; Martini, E.; et al. Albedo Neutron Dosimetry in Germany: Regulations and Performance. *Radiat. Prot. Dosim.* **2014**, *162*, 649–656. [CrossRef]
53. Ahmet, T. Albedo Factor Determination of some Selected 3D Alloy Samples. *Appl. Radiat. Isot.* **2021**, *169*, 109505. [CrossRef]
54. Prabasari, I.; Pettolino, F.; Liao, M.; Bacic, A. Pectic Polysaccharides from Mature Orange (*Citrus Sinensis*) Fruit Albedo Cell Walls: Sequential Extraction and Chemical Characterization. *Carbohyd. Polym.* **2011**, *84*, 484–494. [CrossRef]
55. Sellers, A.; Meadows, A.J. Long-Term Variations in Albedo and Surface-Temperature of Earth. *Nature* **1975**, *254*, 44. [CrossRef]
56. Donohoe, A.; Battisti, D.S. Atmospheric and Surface Contributions to Planetary Albedo. *J. Clim.* **2011**, *24*, 4402–4418. [CrossRef]
57. Lawrence, M.G.; Crutzen, P.J. Was Breaking the Taboo on Research on Climate Engineering via Albedo Modification a Moral Hazard, or a Moral Imperative? *Earths Future* **2017**, *5*, 136–143. [CrossRef]
58. Garfield, E. From the Science of Science to Scientometrics Visualizing the History of Science with HistCite Software. *J. Informetr.* **2009**, *3*, 173–179. [CrossRef]
59. Taha, H. Urban Climates and Heat Islands: Albedo, Evapotranspiration, and Anthropogenic Heat. *Energy Build.* **1997**, *25*, 99–103. [CrossRef]
60. Betts, R.A. Offset of the Potential Carbon Sink from Boreal Forestation by Decreases in Surface Albedo. *Nature* **2000**, *408*, 187–190. [CrossRef]
61. Charney, J.; Quirk, W.J.; Chow, S.H.; Kornfield, J. Comparative-Study of Effects of Albedo Change on Drought in Semi-Arid Regions. *J. Atmos. Sci.* **1977**, *34*, 1366–1385. [CrossRef]
62. Perovich, D.K.; Light, B.; Eicken, H.; Jones, K.F.; Runciman, K.; Nghiem, S.V. Increasing Solar Heating of the Arctic Ocean and Adjacent Seas, 1979-2005: Attribution and Role in the Ice-Albedo Feedback. *Geophys. Res. Lett.* **2007**, *34*, L19505. [CrossRef]
63. Payne, R.E. Albedo of Sea-Surface. *J. Atmos. Sci.* **1972**, *29*, 959. [CrossRef]
64. Hansen, J.; Nazarenko, L. Soot Climate Forcing Via Snow and Ice Albedos. *Proc. Natl. Acad. Sci. USA* **2004**, *101*, 423–428. [CrossRef] [PubMed]
65. Wiscombe, W.J.; Warren, S.G. A Model for the Spectral Albedo of Snow 1. Pure Snow. *J. Atmos. Sci.* **1980**, *37*, 2712–2733. [CrossRef]
66. Zhang, X.; Jiao, Z.; Zhao, C.; Guo, J.; Zhu, Z.; Liu, Z.; Dong, Y.; Yin, S.; Zhang, H.; Cui, L.; et al. Evaluation of BRDF Information Retrieved from Time-Series Multiangle Data of the Himawari-8 AHI. *Remote Sens.* **2022**, *14*, 139. [CrossRef]
67. Jiao, Z.; Zhang, X.; Breon, F.M.; Dong, Y.; Schaaf, C.B.; Roman, M.O.; Wang, Z.; Cui, L.; Yin, S.; Ding, A.; et al. The Influence of Spatial Resolution on the Angular Variation Patterns of Optical Reflectance as Retrieved from MODIS and POLDER Measurements. *Remote Sens. Environ.* **2018**, *215*, 371–385. [CrossRef]
68. Cereceda-Balic, F.; Vidal, V.; Florencia Ruggeri, M.; Gonzalez, H.E. Black Carbon Pollution in Snow and its Impact on Albedo near the Chilean Stations on the Antarctic Peninsula: First Results. *Sci. Total Environ.* **2020**, *743*, 140801. [CrossRef] [PubMed]
69. Leonardi, S.; Magnani, F.; Nole, A.; Van Noije, T.; Borghetti, M. A Global Assessment of Forest Surface Albedo and its Relationships with Climate and Atmospheric Nitrogen Deposition. *Glob. Chang. Biol.* **2015**, *21*, 287–298. [CrossRef] [PubMed]
70. Moody, E.G.; King, M.D.; Schaaf, C.B.; Hall, D.K.; Platnick, S. Northern Hemisphere Five-Year Average (2000–2004) Spectral Albedos of Surfaces in the Presence of Snow: Statistics Computed from Terra MODIS Land Products. *Remote Sens. Environ.* **2007**, *111*, 337–345. [CrossRef]

71. Thomas, C.G.; Donald, K.P. Seasonal and Spatial Evolution of Albedo in a Snow-Ice-Land-Ocean Environment. *J. Geophys. Res.-Ocean.* **2004**, *109*, 1–15.
72. Yoon, J.; Chang, D.Y.; Lelieveld, J.; Pozzer, A.; Kim, J.; Yum, S.S. Empirical Evidence of a Positive Climate Forcing of Aerosols at Elevated Albedo. *Atmos. Res.* **2019**, *229*, 269–279. [CrossRef]
73. Bauer, S.E.; Menon, S. Aerosol Direct, Indirect, Semidirect, and Surface Albedo Effects from Sector Contributions Based on the IPCC AR5 Emissions for Preindustrial and Present-Day Conditions. *J. Geophys. Res.-Atmos.* **2012**, *117*, D1206. [CrossRef]
74. He, M.; Hu, Y.; Chen, N.; Wang, D.; Huang, J.; Stamnes, K. High Cloud Coverage over Melted Areas Dominates the Impact of Clouds on the Albedo Feedback in the Arctic. *Sci. Rep.* **2019**, *9*, 9529. [CrossRef]
75. Ding, A.; Ma, H.; Liang, S.; He, T. Extension of the Hapke Model to the Spectral Domain to Characterize Soil Physical Properties. *Remote Sens. Environ.* **2022**, *269*, 112843. [CrossRef]
76. Widlowski, J.L.; Mio, C.; Disney, M.; Adams, J.; Andredakis, I.; Atzberger, C.; Brennan, J.; Busetto, L.; Chelle, M.; Ceccherini, G.; et al. The Fourth Phase of the Radiative Transfer Model Intercomparison (RAMI) Exercise: Actual Canopy Scenarios and Conformity Testing. *Remote Sens. Environ.* **2015**, *169*, 418–437. [CrossRef]
77. Kokhanovsky, A.A.; Zege, E.P. Scattering Optics of Snow. *Appl. Optics* **2004**, *43*, 1589–1602. [CrossRef] [PubMed]
78. Aoki, T.; Aoki, T.; Fukabori, M.; Hachikubo, A.; Tachibana, Y.; Nishio, F. Effects of Snow Physical Parameters on Spectral Albedo and Bidirectional Reflectance of Snow Surface. *J. Geophys. Res.-Atmos.* **2000**, *105*, 10219–10236. [CrossRef]
79. Jiao, Z.; Ding, A.; Kokhanovsky, A.; Schaaf, C.; Breon, F.; Dong, Y.; Wang, Z.; Liu, Y.; Zhang, X.; Yin, S.; et al. Development of a Snow Kernel to Better Model the Anisotropic Reflectance of Pure Snow in a Kernel-Driven BRDF Model Framework. *Remote Sens. Environ.* **2019**, *221*, 198–209. [CrossRef]
80. Wen, J.; Zhao, X.; Liu, Q.; Tang, Y.; Dou, B. An Improved Land-Surface Albedo Algorithm with DEM in Rugged Terrain. *IEEE Geosci. Remote Sens.* **2014**, *11*, 883–887.
81. Song, J. Diurnal Asymmetry in Surface Albedo. *Agric. For. Meteorol.* **1998**, *92*, 181–189. [CrossRef]
82. Roman, M.O.; Gatebe, C.K.; Schaaf, C.B.; Poudyal, R.; Wang, Z.S.; King, M.D. Variability in Surface BRDF at Different Spatial Scales (30 M-500 M) over a Mixed Agricultural Landscape as Retrieved from Airborne and Satellite Spectral Measurements. *Remote Sens. Environ.* **2011**, *115*, 2184–2203. [CrossRef]
83. Oguntunde, P.G.; Ajayi, A.E.; van de Giesen, N. Tillage and Surface Moisture Effects on Bare-Soil Albedo of a Tropical Loamy Sand. *Soil Till. Res.* **2006**, *85*, 107–114. [CrossRef]
84. Cierniewski, J.; Karnieli, A.; Kazmierowski, C.; Krolewicz, S.; Piekarczyk, J.; Lewinska, K.; Goldberg, A.; Wesolowski, R.; Orzechowski, M. Effects of Soil Surface Irregularities on the Diurnal Variation of Soil Broadband Blue-Sky Albedo. *IEEE J.-STARS* **2015**, *8*, 493–502. [CrossRef]
85. Kala, J.; Evans, J.P.; Pitman, A.J.; Schaaf, C.B.; Decker, M.; Carouge, C.; Mocko, D.; Sun, Q. Implementation of a Soil Albedo Scheme in the CABLEv1.4B Land Surface Model and Evaluation Against MODIS Estimates over Australia. *Geosci. Model Dev.* **2014**, *7*, 2121–2140. [CrossRef]
86. Sanchez-Mejia, Z.M.; Papuga, S.A.; Swetish, J.B.; Van Leeuwen, W.J.D.; Szutu, D.; Hartfield, K. Quantifying the Influence of Deep Soil Moisture on Ecosystem Albedo: The Role of Vegetation. *Water Resour. Res.* **2014**, *50*, 4038–4053. [CrossRef]
87. Fujimaki, H.; Shiozawa, S.; Inoue, M. Effect of Salty Crust on Soil Albedo. *Agric. For. Meteorol.* **2003**, *118*, 125–135. [CrossRef]
88. Xiao, B.; Bowker, M.A. Moss-Biocrusts Strongly Decrease Soil Surface Albedo, Altering Land-Surface Energy Balance in a Dryland Ecosystem. *Sci. Total Environ.* **2020**, *741*, 140425. [CrossRef]
89. Usowicz, B.; Lipiec, J.; Lukowski, M.; Marczewski, W.; Usowicz, J. The Effect of Biochar Application on Thermal Properties and Albedo of Loess Soil under Grassland and Fallow. *Soil Till. Res.* **2016**, *164*, 45–51. [CrossRef]
90. Bozzi, E.; Genesio, L.; Toscano, P.; Pieri, M.; Miglietta, F. Mimicking Biochar-Albedo Feedback in Complex Mediterranean Agricultural Landscapes. *Environ. Res. Lett.* **2015**, *10*, 84014. [CrossRef]
91. Meyer, S.; Bright, R.M.; Fischer, D.; Schulz, H.; Glaser, B. Albedo Impact on the Suitability of Biochar Systems to Mitigate Global Warming. *Environ. Sci. Technol.* **2012**, *46*, 12726–12734. [CrossRef]
92. Aoki, T.; Mikami, M.; Yamazaki, A.; Yabuki, S.; Yamada, Y.; Ishizuka, M.; Zeng, F.J.; Gao, W.D.; Sun, J.Y.; Liu, L.C.; et al. Spectral Albedo of Desert Surfaces Measured in Western and Central China. *J. Meteorol. Soc. Jpn.* **2005**, *83*, 279–290. [CrossRef]
93. Bright, R.M.; Bogren, W.; Bernier, P.; Astrup, R. Carbon-Equivalent Metrics for Albedo Changes in Land Management Contexts: Relevance of the Time Dimension. *Ecol. Appl.* **2016**, *26*, 1868–1880. [CrossRef]
94. Ollinger, S.V.; Richardson, A.D.; Martin, M.E.; Hollinger, D.Y.; Frolking, S.E.; Reich, P.B.; Plourde, L.C.; Katul, G.G.; Munger, J.W.; Oren, R.; et al. Canopy Nitrogen, Carbon Assimilation, and Albedo in Temperate and Boreal Forests: Functional Relations and Potential Climate Feedbacks. *Proc. Natl. Acad. Sci. USA* **2008**, *105*, 19336–19341. [CrossRef] [PubMed]
95. Halim, M.A.; Chen, H.Y.H.; Thomas, S.C. Stand Age and Species Composition Effects on Surface Albedo in a Mixedwood Boreal Forest. *Biogeosciences* **2019**, *16*, 4357–4375. [CrossRef]
96. Yan, H.; Wang, S.; Dai, J.; Wang, J.; Chen, J.; Shugart, H.H. Forest Greening Increases Land Surface Albedo during the Main Growing Period between 2002 and 2019 in China. *J. Geophys. Res.-Atmos.* **2021**, *126*, e2020J–e33582J. [CrossRef]
97. Alibakhshi, S.; Naimi, B.; Hovi, A.; Crowther, T.W.; Rautiainen, M. Quantitative Analysis of the Links between Forest Structure and Land Surface Albedo on a Global Scale. *Remote Sens. Environ.* **2020**, *246*, 111854. [CrossRef]
98. Lukes, P.; Stenberg, P.; Rautiainen, M. Relationship between Forest Density and Albedo in the Boreal Zone. *Ecol. Model.* **2013**, *261*, 74–79. [CrossRef]

99. Kuusinen, N.; Tomppo, E.; Shuai, Y.; Berninger, F. Effects of Forest Age on Albedo in Boreal Forests Estimated from MODIS and Landsat Albedo Retrievals. *Remote Sens. Environ.* **2014**, *145*, 145–153. [CrossRef]
100. Ridgwell, A.; Singarayer, J.S.; Hetherington, A.M.; Valdes, P.J. Tackling Regional Climate Change by Leaf Albedo Bio-Geoengineering. *Curr. Biol.* **2009**, *19*, 146–150. [CrossRef]
101. Hollinger, D.Y.; Ollinger, S.V.; Richardson, A.D.; Meyers, T.P.; Dail, D.B.; Martin, M.E.; Scott, N.A.; Arkebauer, T.J.; Baldocchi, D.D.; Clark, K.L.; et al. Albedo Estimates for Land Surface Models and Support for a New Paradigm Based on Foliage Nitrogen Concentration. *Glob. Chang. Biol.* **2010**, *16*, 696–710. [CrossRef]
102. Riihela, A.; Manninen, T. Measuring the Vertical Albedo Profile of a Subarctic Boreal Forest Canopy. *Silva Fenn.* **2008**, *42*, 807–815. [CrossRef]
103. Rautiainen, M.; Mottus, M.; Yanez-Rausell, L.; Homolova, L.; Malenovsky, Z.; Schaepman, M.E. A Note on Upscaling Coniferous Needle Spectra to Shoot Spectral Albedo. *Remote Sens. Environ.* **2012**, *117*, 469–474. [CrossRef]
104. Zheng, L.; Zhao, G.; Dong, J.; Ge, Q.; Tao, J.; Zhang, X.; Qi, Y.; Doughty, R.B.; Xiao, X. Spatial, Temporal, and Spectral Variations in Albedo Due to Vegetation Changes in China's Grasslands. *ISPRS J. Photogramm.* **2019**, *152*, 1–12. [CrossRef]
105. Mira, M.; Weiss, M.; Baret, F.; Courault, D.; Hagolle, O.; Gallego-Elvira, B.; Olioso, A. The MODIS (Collection V006) BRDF/albedo Product MCD43D: Temporal Course Evaluated over Agricultural Landscape. *Remote Sens. Environ.* **2015**, *170*, 216–228. [CrossRef]
106. Cai, H.; Wang, J.; Feng, Y.; Wang, M.; Qin, Z.; Dunn, J.B. Consideration of Land Use Change-Induced Surface Albedo Effects in Life-Cycle Analysis of Biofuels. *Energy Environ. Sci.* **2016**, *9*, 2855–2867. [CrossRef]
107. Loranty, M.M.; Goetz, S.J.; Beck, P.S.A. Tundra Vegetation Effects on pan-Arctic Albedo. *Environ. Res. Lett.* **2011**, *6*, 24014. [CrossRef]
108. Guan, Y.; Lu, H.; Yin, C.; Xue, Y.; Jiang, Y.; Kang, Y.; He, L.; Heiskanen, J. Vegetation Response to Climate Zone Dynamics and its Impacts on Surface Soil Water Content and Albedo in China. *Sci. Total Environ.* **2020**, *747*, 141537. [CrossRef] [PubMed]
109. Teuling, A.J.; Seneviratne, S.I. Contrasting Spectral Changes Limit Albedo Impact on Land-Atmosphere Coupling during the 2003 European Heat Wave. *Geophys. Res. Lett.* **2008**, *35*, L3401. [CrossRef]
110. Iler, A.M.; Walwema, A.S.; Steltzer, H.; Blázquez-Castro, A. Can Flowers Affect Land Surface Albedo and Soil Microclimates? *Int. J. Biometeorol.* **2021**, *65*, 2011–2023. [CrossRef] [PubMed]
111. Warren, S.G.; Wiscombe, W.J. A Model for the Spectral Albedo of Snow 2. Snow Containing Atmospheric Aerosols. *J. Atmos. Sci.* **1980**, *37*, 2734–2745. [CrossRef]
112. Marshall, S.; Oglesby, R.J. An Improved Snow Hydrology for GCMs 1. Snow Cover Fraction, Albedo, Grain-Size, and Age. *Clim. Dyn.* **1994**, *10*, 21–37.
113. Marks, A.A.; King, M.D. The Effect of Snow/Sea Ice Type on the Response of Albedo and Light Penetration Depth (E-Folding Depth) to Increasing Black Carbon. *Cryosphere* **2014**, *8*, 1625–1638. [CrossRef]
114. Gallet, J.; Domine, F.; Arnaud, L.; Picard, G.; Savarino, J. Vertical Profile of the Specific Surface Area and Density of the Snow at Dome C and on a Transect to Dumont D'Urville, Antarctica—Albedo Calculations and Comparison to Remote Sensing Products. *Cryosphere* **2011**, *5*, 631–649. [CrossRef]
115. Lhermitte, S.; Abermann, J.; Kinnard, C. Albedo over Rough Snow and Ice Surfaces. *Cryosphere* **2014**, *8*, 1069–1086. [CrossRef]
116. Huovinen, P.; Ramirez, J.; Gomez, I. Remote Sensing of Albedo-Reducing Snow Algae and Impurities in the Maritime Antarctica. *ISPRS J. Photogramm. Remote Sens.* **2018**, *146*, 507–517. [CrossRef]
117. Zhang, Y.; Gao, T.; Kang, S.; Shangguan, D.; Luo, X. Albedo Reduction as an Important Driver for Glacier Melting in Tibetan Plateau and its Surrounding Areas. *Earth-Sci. Rev.* **2021**, *220*, 103735. [CrossRef]
118. Hadley, O.L.; Kirchstetter, T.W. Black-Carbon Reduction of Snow Albedo. *Nat. Clim. Chang.* **2012**, *2*, 437–440. [CrossRef]
119. Riihela, A.; Manninen, T.; Laine, V. Observed Changes in the Albedo of the Arctic Sea-Ice Zone for the Period 1982-2009. *Nat. Clim. Chang.* **2013**, *3*, 895–898. [CrossRef]
120. Qu, Y.; Liang, S.L.; Liu, Q.; Li, X.J.; Feng, Y.B.; Liu, S.H. Estimating Arctic Sea-Ice Shortwave Albedo from MODIS Data. *Remote Sens. Environ.* **2016**, *186*, 32–46. [CrossRef]
121. Seo, M.; Lee, C.S.; Kim, H.; Huh, M.; Han, K. Relationship between Sea Ice Concentration and Sea Ice Albedo over Antarctica. *Korean J. Remote Sens.* **2015**, *31*, 347–351. [CrossRef]
122. Applegate, P.J.; Keller, K. How Effective is Albedo Modification (Solar Radiation Management Geoengineering) in Preventing Sea-Level Rise from the Greenland Ice Sheet? *Environ. Res. Lett.* **2015**, *10*, 84018. [CrossRef]
123. Yallop, M.L.; Anesio, A.M.; Perkins, R.G.; Cook, J.; Telling, J.; Fagan, D.; MacFarlane, J.; Stibal, M.; Barker, G.; Bellas, C.; et al. Photophysiology and Albedo-Changing Potential of the Ice Algal Community on the Surface of the Greenland Ice Sheet. *ISME J.* **2012**, *6*, 2302–2313. [CrossRef]
124. Greuell, W.; Knap, W.H. Remote Sensing of the Albedo and Detection of the Slush Line on the Greenland Ice Sheet. *J. Geophys. Res.-Atmos.* **2000**, *105*, 15567–15576. [CrossRef]
125. Leidman, S.Z.; Rennermalm, A.K.; Muthyala, R.; Guo, Q.; Overeem, I. The Presence and Widespread Distribution of Dark Sediment in Greenland Ice Sheet Supraglacial Streams Implies Substantial Impact of Microbial Communities on Sediment Deposition and Albedo. *Geophys. Res. Lett.* **2021**, *48*, L88444. [CrossRef]
126. Tedstone, A.J.; Cook, J.M.; Williamson, C.J.; Hofer, S.; McCutcheon, J.; Irvine-Fynn, T.; Gribbin, T.; Tranter, M. Algal Growth and Weathering Crust State Drive Variability in Western Greenland Ice Sheet Ice Albedo. *Cryosphere* **2020**, *14*, 521–538. [CrossRef]

127. Leshkevich, G.A. Machine Classification of Fresh-Water Ice Types from Landsat-1 Digital Data Using Ice Albedos as Training Sets. *Remote Sens. Environ.* **1985**, *17*, 251–263. [CrossRef]
128. Lu, P.; Lepparanta, M.; Cheng, B.; Li, Z. Influence of Melt-Pond Depth and Ice Thickness on Arctic Sea-Ice Albedo and Light Transmittance. *Cold Reg. Sci. Technol.* **2016**, *124*, 1–10. [CrossRef]
129. Carns, R.C.; Brandt, R.E.; Warren, S.G. Salt Precipitation in Sea Ice and its Effect on Albedo, with Application to Snowball Earth. *J. Geophys. Res.-Ocean.* **2015**, *120*, 7400–7412. [CrossRef]
130. Moeller, R.; Dagsson-Waldhauserova, P.; Moeller, M.; Kukla, P.A.; Schneider, C.; Gudmundsson, M.T. Persistent Albedo Reduction on Southern Icelandic Glaciers Due to Ashfall from the 2010 Eyjafjallajokull Eruption. *Remote Sens. Environ.* **2019**, *233*, 111396. [CrossRef]
131. Gabbi, J.; Huss, M.; Bauder, A.; Cao, F.; Schwikowski, M. The Impact of Saharan Dust and Black Carbon on Albedo and Long-Term Mass Balance of an Alpine Glacier. *Cryosphere* **2015**, *9*, 1385–1400. [CrossRef]
132. Williamson, S.N.; Menounos, B. The Influence of Forest Fires Aerosol and Air Temperature on Glacier Albedo, Western North America. *Remote Sens. Environ.* **2021**, *267*, 112732. [CrossRef]
133. Feng, Y.; Liu, Q.; Qu, Y.; Liang, S. Estimation of the Ocean Water Albedo from Remote Sensing and Meteorological Reanalysis Data. *IEEE Trans. Geosci. Remote Sens.* **2016**, *54*, 850–868. [CrossRef]
134. Seferian, R.; Baek, S.; Boucher, O.; Dufresne, J.; Decharme, B.; Saint-Martin, D.; Roehrig, R. An Interactive Ocean Surface Albedo Scheme (OSAv1.0): Formulation and Evaluation in ARPEGE-Climat (V6.1) and LMDZ (V5A). *Geosci. Model Dev.* **2018**, *11*, 321–338. [CrossRef]
135. Sinnett, G.; Feddersen, F. The Competing Effects of Breaking Waves on Surfzone Heat Fluxes: Albedo versus Wave Heating. *J. Geophys. Res.-Ocean.* **2018**, *123*, 7172–7184. [CrossRef]
136. Crook, J.A.; Jackson, L.S.; Forster, P.M. Can Increasing Albedo of Existing Ship Wakes Reduce Climate Change? *J. Geophys. Res.-Atmos.* **2016**, *121*, 1549–1558. [CrossRef]
137. Wohlfahrt, G.; Tomelleri, E.; Hammerle, A. The Albedo-Climate Penalty of Hydropower Reservoirs. *Nature Energy* **2021**, *6*, 372–377. [CrossRef] [PubMed]
138. Argaman, E.; Keesstra, S.D.; Zeiliguer, A. Monitoring the Impact of Surface Albedo on a Saline Lake in SW Russia. *Land Degrad. Dev.* **2012**, *23*, 398–408. [CrossRef]
139. McMahon, A.; Moore, R.D. Influence of Turbidity and Aeration on the Albedo of Mountain Streams. *Hydrol. Process.* **2017**, *31*, 4477–4491. [CrossRef]
140. Groleau, D.; Mestayer, P.G. Urban Morphology Influence on Urban Albedo: A Revisit with the SOLENE Model. *Bound.-Lay. Meteorol.* **2013**, *147*, 301–327. [CrossRef]
141. Yang, X.; Li, Y. The Impact of Building Density and Building Height Heterogeneity on Average Urban Albedo and Street Surface Temperature. *Build. Environ.* **2015**, *90*, 146–156. [CrossRef]
142. Morini, E.; Castellani, B.; Presciutti, A.; Anderini, E.; Filipponi, M.; Nicolini, A.; Rossi, F. Experimental Analysis of the Effect of Geometry and Facade Materials on Urban District's Equivalent Albedo. *Sustainability* **2017**, *9*, 1245. [CrossRef]
143. Yuan, J.; Farnham, C.; Emura, K. Development of a Retro-Reflective Material as Building Coating and Evaluation on Albedo of Urban Canyons and Building Heat Loads. *Energy Build.* **2015**, *103*, 107–117. [CrossRef]
144. Levinson, R.; Egolf, M.; Chen, S.; Berdahl, P. Experimental Comparison of Pyranometer, Reflectometer, and Spectrophotometer Methods for the Measurement of Roofing Product Albedo. *Sol. Energy* **2020**, *206*, 826–847. [CrossRef]
145. Ramamurthy, P.; Sun, T.; Rule, K.; Bou-Zeid, E. The Joint Influence of Albedo and Insulation on Roof Performance: An Observational Study. *Energy Build.* **2015**, *93*, 249–258. [CrossRef]
146. Chen, J.; Zhou, Z.; Wu, J.; Hou, S.; Liu, M. Field and Laboratory Measurement of Albedo and Heat Transfer for Pavement Materials. *Constr. Build. Mater.* **2019**, *202*, 46–57. [CrossRef]
147. Sen, S.; Roesler, J. Aging Albedo Model for Asphalt Pavement Surfaces. *J. Clean. Prod.* **2016**, *117*, 169–175. [CrossRef]
148. Webster, C.; Jonas, T. Influence of Canopy Shading and Snow Coverage on Effective Albedo in a Snow-Dominated Evergreen Needleleaf Forest. *Remote Sens. Environ.* **2018**, *214*, 48–58. [CrossRef]
149. Manninen, T.; Stenberg, P. Simulation of the Effect of Snow Covered Forest Floor on the Total Forest Albedo. *Agric. For. Meteorol.* **2009**, *149*, 303–319. [CrossRef]
150. Hall, K.; Lindgren, B.S.; Jackson, P. Rock Albedo and Monitoring of Thermal Conditions in Respect of Weathering: Some Expected and some Unexpected Results. *Earth Surf. Proc. Land.* **2005**, *30*, 801–811. [CrossRef]
151. Mohan, S.D.; Davis, F.J.; Badiee, A.; Hadley, P.; Twitchen, C.; Pearson, S.; Gargan, K. Optical and Thermal Properties of Commercial Polymer Film, Modeling the Albedo Effect. *J. Appl. Polym. Sci.* **2021**, *138*, e50581. [CrossRef]
152. Hasan, M.; Ramamoorthi, R. Interactive Albedo Editing in Path-Traced Volumetric Materials. *ACM Trans. Graph.* **2013**, *32*, 1–11. [CrossRef]
153. Jiao, Z.T.; Zhang, H.; Dong, Y.D.; Liu, Q.; Xiao, Q.; Li, X.W. An Algorithm for Retrieval of Surface Albedo from Small View-Angle Airborne Observations through the Use of BRDF Archetypes as Prior Knowledge. *IEEE J.-STARS* **2015**, *8*, 3279–3293. [CrossRef]
154. Canisius, F.; Wang, S.; Croft, H.; Leblanc, S.G.; Russell, H.A.J.; Chen, J.; Wang, R. A UAV-Based Sensor System for Measuring Land Surface Albedo: Tested over a Boreal Peatland Ecosystem. *Drones* **2019**, *3*, 27. [CrossRef]
155. Liu, F.; Chen, Y.; Lu, H.; Shao, H. Albedo Indicating Land Degradation Around the Badain Jaran Desert for Better Land Resources Utilization. *Sci. Total Environ.* **2017**, *578*, 67–73. [CrossRef] [PubMed]

156. Potter, S.; Solvik, K.; Erb, A.; Goetz, S.J.; Johnstone, J.F.; Mack, M.C.; Randerson, J.T.; Roman, M.O.; Schaaf, C.L.; Turetsky, M.R.; et al. Climate Change Decreases the Cooling Effect from Postfire Albedo in Boreal North America. *Glob. Chang. Biol.* **2020**, *26*, 1592–1607. [CrossRef] [PubMed]
157. Lintunen, J.; Rautiainen, A. On Physical and Social-Cost-Based CO_2 Equivalents for Transient Albedo-Induced Forcing. *Ecol. Econ.* **2021**, *190*, 107204. [CrossRef]
158. Kirschbaum, M.U.F.; Whitehead, D.; Dean, S.M.; Beets, P.N.; Shepherd, J.D.; Ausseil, A.G.E. Implications of Albedo Changes following Afforestation on the Benefits of Forests as Carbon Sinks. *Biogeosciences* **2011**, *8*, 3687–3696. [CrossRef]
159. Akbari, H.; Menon, S.; Rosenfeld, A. Global Cooling: Increasing World-Wide Urban Albedos to Offset CO_2. *Clim. Chang.* **2009**, *94*, 275–286. [CrossRef]
160. Otterman, J. Baring High-Albedo Soils by Overgrazing—Hypothesized Desertification Mechanism. *Science* **1974**, *186*, 531–533. [CrossRef]
161. Jackson, R.D.; Idso, S.B. Surface Albedo and Desertification. *Science* **1975**, *189*, 1012–1013. [CrossRef]
162. Zhao, Y.; Wang, X.; Novillo, C.J.; Arrogante-Funes, P.; Vazquez-Jimenez, R.; Berdugo, M.; Maestre, F.T. Remotely Sensed Albedo Allows the Identification of Two Ecosystem States Along Aridity Gradients in Africa. *Land Degrad. Dev.* **2019**, *30*, 1502–1515. [CrossRef]
163. Courel, M.F.; Kandel, R.S.; Rasool, S.I. Surface Albedo and the Sahel Drought. *Nature* **1984**, *307*, 528–531. [CrossRef]
164. Myhre, G.; Govaerts, Y.; Haywood, J.M.; Berntsen, T.K.; Lattanzio, A. Radiative Effect of Surface Albedo Change from Biomass Burning. *Geophys. Res. Lett.* **2005**, *32*, L20812. [CrossRef]
165. Meunier, F.; Visser, M.D.; Shiklomanov, A.; Dietze, M.C.; Guzman, J.A.Q.; Sanchez-Azofeifa, G.A.; De Deurwaerder, H.P.T.; Moorthy, S.M.K.; Schnitzer, S.A.; Marvin, D.C.; et al. Liana Optical Traits Increase Tropical Forest Albedo and Reduce Ecosystem Productivity. *Glob. Chang. Biol.* **2022**, *28*, 227–244. [CrossRef] [PubMed]
166. Flanner, M.G.; Shell, K.M.; Barlage, M.; Perovich, D.K.; Tschudi, M.A. Radiative Forcing and Albedo Feedback from the Northern Hemisphere Cryosphere between 1979 and 2008. *Nat. Geosci.* **2011**, *4*, 151–155. [CrossRef]
167. Wang, Z.; Erb, A.M.; Schaaf, C.B.; Sun, Q.; Liu, Y.; Yang, Y.; Shuai, Y.; Casey, K.A.; Roman, M.O. Early Spring Post-Fire Snow Albedo Dynamics in High Latitude Boreal Forests Using Landsat-8 OLI Data. *Remote Sens. Environ.* **2016**, *185*, 71–83. [CrossRef]
168. Chen, D.; Loboda, T.V.; He, T.; Zhang, Y.; Liang, S. Strong Cooling Induced by Stand-Replacing Fires through Albedo in Siberian Larch Forests. *Sci. Rep.* **2018**, *8*, 4821. [CrossRef]
169. Scherrer, S.C.; Ceppi, P.; Croci-Maspoli, M.; Appenzeller, C. Snow-Albedo Feedback and Swiss Spring Temperature Trends. *Theor. Appl. Climatol.* **2012**, *110*, 509–516. [CrossRef]
170. Molotch, N.P.; Bales, R.C. Comparison of Ground-Based and Airborne Snow Surface Albedo Parameterizations in an Alpine Watershed: Impact on Snowpack Mass Balance. *Water Resour. Res.* **2006**, *42*, W5410. [CrossRef]
171. Williamson, S.N.; Copland, L.; Thomson, L.; Burgess, D. Comparing Simple Albedo Scaling Methods for Estimating Arctic Glacier Mass Balance. *Remote Sens. Environ.* **2020**, *246*, 111858. [CrossRef]
172. Lenaerts, J.T.M.; Lhermitte, S.; Drews, R.; Ligtenberg, S.R.M.; Berger, S.; Helm, V.; Smeets, C.J.P.P.; Van den Broeke, M.R.; Van de Berg, W.J.; Van Meijgaard, E.; et al. Meltwater Produced by Wind-Albedo Interaction Stored in an East Antarctic Ice Shelf. *Nat. Clim. Chang.* **2017**, *7*, 58. [CrossRef]
173. Allen, R.J.; Zender, C.S. Effects of Continental-Scale Snow Albedo Anomalies on the Wintertime Arctic Oscillation. *J. Geophys. Res.-Atmos.* **2010**, *115*, D23105. [CrossRef]
174. Picard, G.; Domine, F.; Krinner, G.; Arnaud, L.; Lefebvre, E. Inhibition of the Positive Snow-Albedo Feedback by Precipitation in Interior Antarctica. *Nat. Clim. Chang.* **2012**, *2*, 795–798. [CrossRef]
175. Riihela, A.; Bright, R.M.; Anttila, K. Recent Strengthening of Snow and Ice Albedo Feedback Driven by Antarctic Sea-Ice Loss. *Nat. Geosci.* **2021**, *14*, 832. [CrossRef]
176. Beck, P.S.A.; Goetz, S.J.; Mack, M.C.; Alexander, H.D.; Jin, Y.; Randerson, J.T.; Loranty, M.M. The Impacts and Implications of an Intensifying Fire Regime on Alaskan Boreal Forest Composition and Albedo. *Glob. Chang. Biol.* **2011**, *17*, 2853–2866. [CrossRef]
177. Gnanamoorthy, P.; Song, Q.; Zhao, J.; Zhang, Y.; Liu, Y.; Zhou, W.; Sha, L.; Fan, Z.; Burman, P.K.D. Altered Albedo Dominates the Radiative Forcing Changes in a Subtropical Forest Following an Extreme Snow Event. *Glob. Chang. Biol.* **2021**, *27*, 6192–6205. [CrossRef]
178. Vanderhoof, M.Y.; Williams, C.A.; Shuai, Y.; Jarvis, D.; Kulakowski, D.; Masek, J. Albedo-Induced Radiative Forcing from Mountain Pine Beetle Outbreaks in Forests, South-Central Rocky Mountains: Magnitude, Persistence, and Relation to Outbreak Severity. *Biogeosciences* **2014**, *11*, 563–575. [CrossRef]
179. Craft, K.M.; Horel, J.D. Variations in Surface Albedo Arising from Flooding and Desiccation Cycles on the Bonneville Salt Flats, Utah. *J. Appl. Meteorol. Clim.* **2019**, *58*, 773–785. [CrossRef]
180. Murphree, J.S.; Anger, C.D. An Empirical-Method for Determining Albedo Contribution to Satellite Photometer Data. *Remote Sens. Environ.* **1980**, *9*, 183–187. [CrossRef]
181. Wallner, S.; Kocifaj, M. Impacts of Surface Albedo Variations on the Night Sky Brightness—A Numerical and Experimental Analysis. *J. Quant. Spectrosc. Radiat. Transf.* **2019**, *239*, 106648. [CrossRef]
182. Hu, Y.; Hou, M.; Zhao, C.; Zhen, X.; Yao, L.; Xu, Y. Human-Induced Changes of Surface Albedo in Northern China from 1992-2012. *Int. J. Appl. Earth Obs. Geoinf.* **2019**, *79*, 184–191. [CrossRef]

183. Giambelluca, T.W.; Holscher, D.; Bastos, T.X.; Frazao, R.R.; Nullet, M.A.; Ziegler, A.D. Observations of Albedo and Radiation Balance over Postforest Land Surfaces in the Eastern Amazon Basin. *J. Clim.* **1997**, *10*, 919–928. [CrossRef]
184. Bright, R.M.; Stromman, A.H.; Peters, G.P. Radiative Forcing Impacts of Boreal Forest Biofuels: A Scenario Study for Norway in Light of Albedo. *Environ. Sci. Technol.* **2011**, *45*, 7570–7580. [CrossRef] [PubMed]
185. Kreidenweis, U.; Humpenoeder, F.; Stevanovic, M.; Bodirsky, B.L.; Kriegler, E.; Lotze-Campen, H.; Popp, A. Afforestation to Mitigate Climate Change: Impacts on Food Prices under Consideration of Albedo Effects. *Environ. Res. Lett.* **2016**, *11*, 85001. [CrossRef]
186. Cohen, J.Y.; Pulliainen, J.; Menard, C.B.; Johansen, B.; Oksanen, L.; Luojus, K.; Ikonen, J. Effect of Reindeer Grazing on Snowmelt, Albedo and Energy Balance Based on Satellite Data Analyses. *Remote Sens. Environ.* **2013**, *135*, 107–117. [CrossRef]
187. Myhre, G.; Kvalevag, M.M.; Schaaf, C.B. Radiative Forcing Due to Anthropogenic Vegetation Change Based on MODIS Surface Albedo Data. *Geophys. Res. Lett.* **2005**, *32*, L21410. [CrossRef]
188. Song, Y.; Lv, M.; Wang, M.; Li, X.; Qu, Y. Reconstruction of Historical Land Surface Albedo Changes in China from 850 to 2015 Using Land Use Harmonization Data and Albedo Look-Up Maps. *Earth Space Sci.* **2021**, *8*, e2021EA001799. [CrossRef]
189. Dong, N.; Luo, M.; Liu, Z.; Sun, J.; Wu, K.; Lin, H. The Roles of Leaf Area Index and Albedo in Vegetation Induced Temperature Changes across China Using Modelling and Observations. *Clim. Dyn.* **2021**, 1–17. [CrossRef]
190. Tang, R.; Zhao, X.; Zhou, T.; Jiang, B.; Wu, D.; Tang, B. Assessing the Impacts of Urbanization on Albedo in Jing-Jin-Ji Region of China. *Remote Sens.* **2018**, *10*, 1096. [CrossRef]
191. Trlica, A.; Hutyra, L.R.; Schaaf, C.L.; Erb, A.; Wang, J.A. Albedo, Land Cover, and Daytime Surface Temperature Variation across an Urbanized Landscape. *Earths Future* **2017**, *5*, 1084–1101. [CrossRef]
192. Susca, T. Enhancement of Life Cycle Assessment (LCA) Methodology to Include the Effect of Surface Albedo on Climate Change: Comparing Black and White Roofs. *Environ. Pollut.* **2012**, *163*, 48–54. [CrossRef]
193. Yu, B.; Lu, Q. Estimation of Albedo Effect in Pavement Life Cycle Assessment. *J. Clean. Prod.* **2014**, *64*, 306–309. [CrossRef]
194. Acharya, T.; Riehl, B.; Fuchs, A. Effects of Albedo and Thermal Inertia on Pavement Surface Temperatures with Convective Boundary Conditions–A CFD Study. *Processes* **2021**, *9*, 2078. [CrossRef]
195. Schrijvers, P.J.C.; Jonker, H.J.J.; de Roode, S.R.; Kenjeres, S. The Effect of Using a High-Albedo Material on the Universal Temperature Climate Index within a Street Canyon. *Urban Clim.* **2016**, *17*, 284–303. [CrossRef]
196. Samson, G.; Masson, S.; Durand, F.; Terray, P.; Berthet, S.; Jullien, S. Roles of Land Surface Albedo and Horizontal Resolution on the Indian Summer Monsoon Biases in a Coupled Ocean-Atmosphere Tropical-Channel Model. *Clim. Dyn.* **2017**, *48*, 1571–1594. [CrossRef]
197. Covey, C.; Taylor, K.E.; Dickinson, R.E. Upper Limit for Sea Ice Albedo Feedback Contribution to Global Warming. *J. Geophys. Res.-Atmos.* **1991**, *96*, 9169–9174. [CrossRef]
198. Romanova, V.; Lohmann, G.; Grosfeld, K. Effect of Land Albedo, CO_2, Orography, and Oceanic Heat Transport on Extreme Climates. *Clim. Past* **2006**, *2*, 31–42. [CrossRef]
199. Willeit, M.; Ganopolski, A. The Importance of Snow Albedo for Ice Sheet Evolution over the Last Glacial Cycle. *Clim. Past* **2018**, *14*, 697–707. [CrossRef]
200. Fraedrich, K. Catastrophes and Resilience of a Zero-Dimensional Climate System with Ice-Albedo and Greenhouse Feedback. *Q. J. R. Meteorol. Soc.* **1979**, *105*, 147–167. [CrossRef]
201. Graversen, R.G.; Wang, M. Polar Amplification in a Coupled Climate Model with Locked Albedo. *Clim. Dyn.* **2009**, *33*, 629–643. [CrossRef]
202. Graversen, R.G.; Langen, P.L.; Mauritsen, T. Polar Amplification in CCSM4: Contributions from the Lapse Rate and Surface Albedo Feedbacks. *J. Clim.* **2014**, *27*, 4433–4450. [CrossRef]
203. Zeitz, M.; Reese, R.; Beckmann, J.; Krebs-Kanzow, U.; Winkelmann, R. Impact of the Melt-Albedo Feedback on the Future Evolution of the Greenland Ice Sheet with PISM-dEBM-simple. *Cryosphere* **2021**, *15*, 5739–5764. [CrossRef]
204. Wood, A.J.; Ackland, G.J.; Lenton, T.M. Mutation of Albedo and Growth Response Produces Oscillations in a Spatial Daisyworld. *J. Theor. Biol.* **2006**, *242*, 188–198. [CrossRef] [PubMed]
205. Landry, J.; Parrott, L.; Price, D.T.; Ramankutty, N.; Matthews, H.D. Modelling Long-Term Impacts of Mountain Pine Beetle Outbreaks on Merchantable Biomass, Ecosystem Carbon, Albedo, and Radiative Forcing. *Biogeosciences* **2016**, *13*, 5277–5295. [CrossRef]
206. Abell, J.T.; Pullen, A.; Lebo, Z.J.; Kapp, P.; Gloege, L.; Metcalf, A.R.; Nie, J.; Winckler, G. A Wind-Albedo-Wind Feedback Driven by Landscape Evolution. *Nat. Commun.* **2020**, *11*, 96. [CrossRef] [PubMed]
207. Taha, H. Modeling the Impacts of Large-Scale Albedo Changes on Ozone Air Quality in the South Coast Air Basin. *Atmos. Environ.* **1997**, *31*, 1667–1676. [CrossRef]
208. Yuan, J.; Emura, K.; Farnham, C. Is Urban Albedo or Urban Green Covering More Effective for Urbanmicro Climate Improvement?: A Simulation for Osaka. *Sustain. Cities Soc.* **2017**, *32*, 78–86. [CrossRef]
209. Mohammad, P.; Aghlmand, S.; Fadaei, A.; Gachkar, S.; Gachkar, D.; Karimi, A. Evaluating the Role of the Albedo of Material and Vegetation Scenarios along the Urban Street Canyon for Improving Pedestrian Thermal Comfort Outdoors. *Urban Clim.* **2021**, *40*, 100993. [CrossRef]

210. Falasca, S.; Ciancio, V.; Salata, F.; Golasi, I.; Rosso, F.; Curci, G. High Albedo Materials to Counteract Heat Waves in Cities: An Assessment of Meteorology, Buildings Energy Needs and Pedestrian Thermal Comfort. *Build. Environ.* **2019**, *163*, 106242. [CrossRef]
211. Jandaghian, Z.; Berardi, U. Analysis of the Cooling Effects of Higher Albedo Surfaces during Heat Waves Coupling the Weather Research and Forecasting Model with Building Energy Models. *Energy Build.* **2020**, *207*, 109627. [CrossRef]
212. Yin, J.; Zhan, X.; Zheng, Y.; Hain, C.R.; Ek, M.; Wen, J.; Fang, L.; Liu, J. Improving Noah Land Surface Model Performance Using near Real Time Surface Albedo and Green Vegetation Fraction. *Agric. For. Meteorol.* **2016**, *218*, 171–183. [CrossRef]
213. Boussetta, S.; Balsamo, G.; Dutra, E.; Beljaars, A.; Albergel, C. Assimilation of Surface Albedo and Vegetation States from Satellite Observations and their Impact on Numerical Weather Prediction. *Remote Sens. Environ.* **2015**, *163*, 111–126. [CrossRef]
214. Schaeffer, M.; Eickhout, B.; Hoogwijk, M.; Strengers, B.; van Vuuren, D.; Leemans, R.; Opsteegh, T. CO2 and Albedo Climate Impacts of Extratropical Carbon and Biomass Plantations. *Glob. Biogeochem. Cycles* **2006**, *20*, B2020. [CrossRef]
215. Thackeray, C.W.; Hall, A.; Zelinka, M.D.; Fletcher, C.G. Assessing Prior Emergent Constraints on Surface Albedo Feedback in CMIP6. *J. Clim.* **2021**, *34*, 3889–3905. [CrossRef]
216. Vamborg, F.S.E.; Brovkin, V.; Claussen, M. Background Albedo Dynamics Improve Simulated Precipitation Variability in the Sahel Region. *Earth Syst. Dyn.* **2014**, *5*, 89–101. [CrossRef]
217. Voigt, A.; Stevens, B.; Bader, J.; Mauritsen, T. Compensation of Hemispheric Albedo Asymmetries by Shifts of the ITCZ and Tropical Clouds. *J. Clim.* **2014**, *27*, 1029–1045. [CrossRef]
218. Burrett, C.F. Phanerozoic Land Sea and Albedo Variations as Climate Controls. *Nature* **1982**, *296*, 54–56. [CrossRef]
219. Vamborg, F.S.E.; Brovkin, V.; Claussen, M. The Effect of a Dynamic Background Albedo Scheme on Sahel/Sahara Precipitation during the mid-Holocene. *Clim. Past* **2011**, *7*, 117–131. [CrossRef]
220. Yang, J.; Peltier, W.R.; Hu, Y. The Initiation of Modern "Soft Snowball" and "Hard Snowball" Climates in CCSM3. Part I: The Influences of Solar Luminosity, CO2 Concentration, and the Sea Ice/Snow Albedo Parameterization. *J. Clim.* **2012**, *25*, 2711–2736. [CrossRef]
221. Kienert, H.; Feulner, G.; Petoukhov, V. Albedo and Heat Transport in 3-D Model Simulations of the Early Archean Climate. *Clim. Past* **2013**, *9*, 1841–1862. [CrossRef]
222. Howell, F.W.; Haywood, A.M.; Dowsett, H.J.; Pickering, S.J. Sensitivity of Pliocene Arctic Climate to Orbital Forcing, Atmospheric CO_2 and Sea Ice Albedo Parameterisation. *Earth Planet. Sci. Lett.* **2016**, *441*, 133–142. [CrossRef]
223. Lutz, D.A.; Howarth, R.B. The Price of Snow: Albedo Valuation and a Case Study for Forest Management. *Environ. Res. Lett.* **2015**, *10*, 64013. [CrossRef]
224. Favero, A.; Sohngen, B.; Huang, Y.; Jin, Y. Global Cost Estimates of Forest Climate Mitigation with Albedo: A New Integrative Policy Approach. *Environ. Res. Lett.* **2018**, *13*, 125002. [CrossRef]
225. Rautiainen, A.; Lintunen, J.; Uusivuori, J. Market-Level Implications of Regulating Forest Carbon Storage and Albedo for Climate Change Mitigation. *Agric. Resour. Econ. Rev.* **2018**, *47*, 239–271. [CrossRef]
226. Starr, J.; Zhang, J.; Reid, J.S.; Roberts, D.C. Albedo Impacts of Changing Agricultural Practices in the United States through Space-Borne Analysis. *Remote Sens.* **2020**, *12*, 2887. [CrossRef]
227. Drewry, D.T.; Kumar, P.; Long, S.P. Simultaneous Improvement in Productivity, Water Use, and Albedo through Crop Structural Modification. *Glob. Chang. Biol.* **2014**, *20*, 1955–1967. [CrossRef] [PubMed]
228. Davin, E.L.; Seneviratne, S.I.; Ciais, P.; Olioso, A.; Wang, T. Preferential Cooling of Hot Extremes from Cropland Albedo Management. *Proc. Natl. Acad. Sci. USA* **2014**, *111*, 9757–9761. [CrossRef] [PubMed]
229. Holtsmark, B. A Comparison of the Global Warming Effects of Wood Fuels and Fossil Fuels Taking Albedo into Account. *GCB Bioenergy* **2015**, *7*, 984–997. [CrossRef]
230. Abraha, M.; Chen, J.; Hamilton, S.K.; Sciusco, P.; Lei, C.; Shirkey, G.; Yuan, J.; Robertson, G.P. Albedo-Induced Global Warming Impact of Conservation Reserve Program Grasslands Converted to Annual and Perennial Bioenergy Crops. *Environ. Res. Lett.* **2021**, *16*, 84059. [CrossRef]
231. Cereceda-Balic, F.; Vidal, V.; Moosmuller, H.; Lapuerta, M. Reduction of Snow Albedo from Vehicle Emissions at Portillo, Chile. *Cold Reg. Sci. Technol.* **2018**, *146*, 43–52. [CrossRef]
232. Gschnaller, S. The Albedo Loss from the Melting of the Greenland Ice Sheet and the Social Cost of Carbon. *Clim. Chang.* **2020**, *163*, 2201–2231. [CrossRef]
233. Silva, H.I.; Golden, J.S. Spatial Superposition Method via Model Coupling for Urban Heat Island Albedo Mitigation Strategies. *J. Appl. Meteorol. Clim.* **2012**, *51*, 1971–1979. [CrossRef]
234. Arumugam, R.S.; Garg, V.; Ram, V.V.; Bhatia, A. Optimizing Roof Insulation for Roofs with High Albedo Coating and Radiant Barriers in India. *J. Build. Eng.* **2015**, *2*, 52–58. [CrossRef]
235. Tan, C.L.; Wong, N.H.; Tan, P.Y.; Jusuf, S.K.; Chiam, Z.Q. Impact of Plant Evapotranspiration Rate and Shrub Albedo on Temperature Reduction in the Tropical Outdoor Environment. *Build. Environ.* **2015**, *94*, 206–217. [CrossRef]
236. Mekemeche, A.; Beghdad, M. Impact of the Environmental Effective Albedo on the Performance of PERC plus Solar Cells. *Silicon-Neth.* **2021**, *13*, 3991–3998. [CrossRef]
237. Cuevas, A.; Luque, A.; Eguren, J.; Delalamo, J. 50-Percent More Output Power from an Albedo-Collecting Flat Panel Using Bifacial Solar-Cells. *Sol. Energy* **1982**, *29*, 419–420. [CrossRef]

238. Kim, S.; Thanh, T.T.; Park, J.; Duy, P.P.; Lee, S.; Huy, B.D.; Nam, N.D.; Vinh-Ai, D.; Kim, J.; Yi, J. Over 30% Efficiency Bifacial 4-Terminal Perovskite-Heterojunction Silicon Tandem Solar Cells with Spectral Albedo. *Sci. Rep.* **2021**, *11*, 15524. [CrossRef]
239. Sugiura, T.; Matsumoto, S.; Nakano, N. Bifacial Heterojunction Back Contact Solar Cell: 29-MW/cm(2) Output Power Density in Standard Albedo Condition. *IEEE Trans. Electron Devices* **2021**, *68*, 5645–5651. [CrossRef]
240. Fartaria, T.O.; Pereira, M.C. Simulation and Computation of Shadow Losses of Direct Normal, Diffuse Solar Radiation and Albedo in a Photovoltaic Field with Multiple 2-Axis Trackers Using Ray Tracing Methods. *Sol. Energy* **2013**, *91*, 93–101. [CrossRef]
241. Lv, Y.; Fan, D.; Kong, M. Reliability Assessment on PV Backsheets with and without Considering Spectral UV Albedo Effects: A Theoretical Comparison. *Sol. Energy Mater. Sol. Cells* **2021**, *230*, 111230. [CrossRef]
242. Lattanzio, A.; Schulz, J.; Matthews, J.; Okuyama, A.; Theodore, B.; Bates, J.J.; Knapp, K.R.; Kosaka, Y.; Schueller, L. Land Surface Albedo from Geostationary Satellites: A Multiagency Collaboration within SCOPE-CM. *Bull. Am. Meteorol. Soc.* **2013**, *94*, 205–214. [CrossRef]